Expression and purification of the *Streptococcus pyogenes* Cas9 protein for ribonucleoprotein transfection strategy and CRISPR/Cas9-based in AAVS1 safe harbor locus.

Renato André Duarte dos Santos

Thesis to obtain the Master of Science Degree in

Biotechnology

Supervisors:

Dr. Nuno Filipe Santos Bernardes

Prof. Cláudia Alexandra Martins Lobato da Silva

Examination Committee

Chairperson: Prof. Arsénio do Carmo Sales Mendes Fialho

Supervisor: Dr. Nuno Filipe Santos Bernardes

Members of the Committee: Dr. Joana Rita Rodrigues Feliciano

November 2018

Acknowledges

I want to thank Dr.Nuno Bernardes and Prof. Cláudia Lobato for being my supervisors through my thesis and making me a better researcher and professional in the field of Biotechnology by giving me challenges, help, support and knowledge. Marília Silva was a great companion in this research, that supported me greatly through this work and helped me achieve many of the milestones of this thesis. Ana Rita Garizo, thanks for helping me beginning this journey in the lab, and thanks Andreia Pimenta and Joana Feliciano for being always ready to help me in the lab. Thanks to my family I had the chance to study and achieve higher education, but also support in reaching my objectives. Not only from family, but friends also had a great impact in reaching my goals. To all, I thank you.

Funding received by iBB-Institute for Bioengineering and Biosciences from FCT (UID/BIO/04565/2013) and from Programa Operacional Regional de Lisboa 2020 (Project N. 007317) is acknowledged.

Abstract

Mesenchymal Stem Cells (MSCs) present low immunogenicity and tumor tropism, properties essential to turn them anti-cancer drug delivery vehicles by gene editing. Azurin is a bacterial protein capable of reducing tumor proliferation and inducing apoptosis without known effects in normal cells. If engineered to produce azurin, engineered MSCs could became a tool against tumorigenesis with potential for clinical use. The most efficient and specific genetic engineering tool is CRISPR-Cas9. However, when cells' genome is exposed to this tool for long periods, the chance of off-targeting increases, therefore, an approach to produce *in vitro* a CRISPR-Cas9 complex was developed and optimized for efficient gene edition in AAVS1 safe-harbor, with low lifetime inside cells. Cas9 production and purification optimized, resulted in higher and purer Cas9, using *E. coli* culture at 25ºC with 0.2mM IPTG for overexpression induction. Cleavage efficiency of RNP complex formed with the purified protein was tested *in vitro* with DNA from MSC, HEK and HeLa, and in lipo-transfected HEK cells with successful cleavage detected using GeneArt™ Genomic Cleavage Detection Kit. This strategy may represent a more suitable approach for MSCs since all-in-one plasmid approaches present very low levels of success, particularly due to high sensitivity of these cells to the selection with puromycin. Despite optimization of microporation of MSCs with an all-in-one plasmid (optimal conditions: one pulse, 1400V and 1300V, 30ms), the cells died after puromycin selection, reinforcing the need of higher Cas9 protein levels for future studies to access the donor-to-donor variability and tissue source' influence of MSC.

Keywords: CRISPR-Cas9, RNP, Azurin, MSCs, Microporation, Lipofection

Resumo

"Mesenchymal Stem Cells" (MSCs) apresentam baixa imunogenicidade e tropismo tumoral, características essenciais para as transformar em veículos transportadores de agentes anticancerígenos, usando edição genética. Azurina é uma proteína bacteriana capaz de reduzir a replicação e induzir apoptose em células tumorais sem efeitos secundários conhecidos nas células normais. Se geneticamente modificadas para produzir azurina, as "MSCs" poder-se-iam tornar uma ferramenta terapêutica contra a tumurigénese. Atualmente, a ferramenta de edição genómica com maior eficiência e especificidade é o CRISPR-Cas9. Infelizmente, quando células são expostas a este complexo por longos períodos, a chance de "off-targeting" aumenta. Assim, produziu-se *in vitro* o complexo para edição eficiente no "genomic-safe-harbor" AAVS1, e para diminuir o tempo de de residência intracelular. A produção e purificação de Cas9 optimizada resultou numa maior quantidade e pureza de Cas9, usando culturas de *E. coli* a 25ºC com 0.2mM IPTG para indução de super-expressão. A eficiência de clivagem da ribonucleoproteina foi testada i*n vitro* em ADN de células "MSCs", "HEK", HeLa, e em HEK transfectadas por lipofecção. O sucesso da clivagem da cadeia dupla do ADN foi observada usando o Kit de Deteção de Clivagem "GeneArt™ Genomic". Esta estratégia pode ser preferível à modificação das "MSCs" que apresentam baixa edição genómica por plasmídeo único, devido à sensibilidade à seleção com puromicina. Apesar da otimização da microporação (condições ótimas: um pulso,1400V e 1300V, 30ms), as células não resistem à seleção, reforçando a necessidade de obter elevados níveis de Cas9 para estudos futuros de variabilidade entre dadores e tecidos de origem das "MSCs".

Palavras-chave: CRISPR-Cas9, Ribonucleoproteina, Azurina, "MSCs", Microporação, Lipofecção

Table of contents

List of Tables

List of Figures

List of Abbreviations

6His - Six-Histidine tag

Amp - Ampicillin

ATC - Anaplastic Thyroid Cancer

AT-MSCs - Adipose tissue MSCs

ATMP - Advanced Therapy Medicinal Product

BDNF - Brain-Derived Neurotrophic Factor

CAR T cells - Chimeric Antigen Receptor T cells

CML - Chronic Myeloid Leukemia

CRISPR - Clustered Regularly Interspaced Short Palindromic Repeats

crRNA - CRISPR RNA

CV – Column Volume

dCas9 - Dead Cas9

DMD - Duchenne Muscular Dystrophy

DNA - Deoxyribonucleic Acid

DOX - Doxycycline

DSB - Double Strand Break

EDTA - Ethylenediaminetetraacetic acid

ESCs - Embryonic Stem Cells

EU - European Union

gRNA – Guide Ribonucleic Acid

GSHs - Genomic Safe Harbors

HCM - Hypertrophic Cardiomyopathy

HEPES - 4-(2-hydroxyethyl)-1-piperazineethanesulfonic acid

HEK - Human Embryonic Kidney cells

hftMSCs - Human Fallopian Tube MSCs

hiPSC - Human Induced Pluripotent Stem Cells

HLA - Human Leukocyte Antigen

HNRNPL - Heterogeneous Nuclear Ribonucleoprotein L

IEX - Ion-Exchange chromatography

IL - Interleukins

IMAC - Immobilized Metal Affinity Chromatography

InDel - Insertion or Deletion

iPSCs - Induced Pluripotent Stem Cells

IPTG - Isopropyl β-D-1-thiogalactopyranoside

LVs - Lentiviral Vectors

MBP- Maltose-Binding Protein

MSCs – Mesenchymal Stem Cells

mRNA - Messenger RNA

MWCO - Molecular Weight Cut-Off

NHEJ - Non-Homologous End Joining

NP-loaded MSCs – Nanoparticles-loaded MSCs

NSCLC - Non-Small Cell Lung Cancer

OD - Optical Density

PAM - Protospacer-Adjacent Motif

PBS - Phosphate-Buffered Saline

PD1 - Programmed cell Death protein 1

RNP - Ribonucleoprotein

SDS - Sodium Dodecyl Sulfate

SEC - Size-Exclusion Chromatography

sgRNA – Single guide RNA

SMART cells - Stem cells Modified for Autonomous Regenerative Therapy cells

SpCas9- *Streptococcus pyogenes* Cas9

TCR - T cell receptor

TRAIL - Tumor necrosis factor-Related Apoptosis Inducing Ligand

UCB-MSCs - Umbilical Cord Blood MSCs

TALEN - Transcription Activator-Like Effector Nuclease)

TEV - Tobacco Etch Virus

tracrRNA - trans-activating crRNA

ZFN - Zinc Finger Nuclease

1. Introduction

Recent advances in genetics had led the medical field to enroll in the development of gene and cell therapies that show great potential in treatment of genetic, viral, degenerative and oncogenic diseases, comparing with the present standard treatments available to public. The highest enhancer of this field was the discovery of CRISPR-Cas9 system, a ribonucleoprotein complex founded in bacteria and archaeal with the ability to cleave DNA in pre-determined sites of DNA, used in this basis as a unicellular immune system against virus [1].

Using this cleavage capability and high specificity, editing genomes is a reliable reality with the potential to lead to the cure of diseases using genetic material, or engineered cells with drug delivery properties. With a higher prospect for cancer treatment, engineered Mesenchymal Stem/Stromal Cells (MSCs) are a great candidate as it will be showed more forward in this introduction.

1.1. Mesenchymal Stem/Stromal Cells (MSCs)

MSCs are multipotent stem cells with the capability of self-renewal, without significant changes, and differentiation into all mesoderm lineages and some ectoderm and endoderm cells [2]. Some examples of possible outcomes of differentiation into connective tissue lineages are osteocytes, chondrocytes [3], tenocytes [4], adipocytes [5] and smooth muscle cells [6], under certain physiological or experimental conditions. These cells can also differentiate into lineages beyond the mesodermal, such as neurons and astrocytes [7], from the ectodermal lineage, and hepatocytes [8] from the endoderm lineage.

Compared to embryonic stem cells (ESCs), MSCs have a minor potential for replication and differentiation, but using them do not exhibit major ethical concerns since MSCs can be isolated from adult bone marrow and adipose tissue or umbilical cord [9]. Induced pluripotent stem cells (iPSCs) would not present ethical issues towards embryos and differentiation potential would be maintained. However, just like ESCs, iPSCs can form teratomas unlike the MSCs [10,11,12].

MSCs have many features with diverse applications, one in concrete is their unique tropism. Signals of the microenvironment of inflammatory nature, chemoattract MSCs for damaged sites in order for them to act as a reparation system. Such signals can be released due to hypoxia, ischemia, radiation, cutaneous cuts and tumors. This tropism for tumor tissue and injurie sites together with gene editing, can lead to cell therapies for drug delivery at tumors and tissue repair [13].

Another promising characteristic of these cells is their immunomodulatory and anti-inflammatory effects that turns it possible to transplant these cells in humans without the need for MSCs to be from the individual or from an immunocompatible patient thus making the attainment of working cells easier.

This hypoimmunogenicity is due to the inhibition of proliferation and maturation of immune cells and their reactions, low expression of HLA class I, no expression of HLA class Ⅱ and costimulatory molecules like CD40, CD80, and CD86 [14].

MSCs have been already used as regenerative tools [15] and drug delivery mechanisms for treatment of diverse diseases, being one the ilnesses with highest focus, the cancer. Some examples of anti-cancer agents expressed by engineered MSCs used in such strategy are interferons α, β, interleukins 2, 12, chemokine CX3CL1 (US20110027239, US20120087901, WO2012071527), oncolytic viruses or tumor necrosis factor-related apoptosis inducing ligand (TRAIL) (WO2012106281) [16].

Even though MSCs show great potential in medical treatment of diverse diseases including cancer, negative aspects have also been observed. The community has been divided about how MSCs affect tumor progression, since there is evidence of MSCs inhibiting tumor development, but also evidences of stimulatory effects on tumor pathogenesis [17]. Human hepatoma HepG2 cells cocultured with MSCs, treated with conditional media of MSCs *in vitro* and co-injected in nude rats, showed decrease of proliferation and increase of apoptosis of the HepG2 cells [18], while use of conditional media of MSCs in Balb/C mice promoted the invasion and proliferation of colorectal cancer cells [19]. Depending of the tissue of origin of the MSCs, these can stimulate or inhibit cancer. For example, AT-MSCs (Adipose tissue MSCs) induce progression of the glioblastoma cells while UCB-MSCs (umbilical cord blood MSCs) inhibit [20]. Also, it is known that even though, being from the same tissue, MSCs can also have different effects in cancer. hftMSCs (Human fallopian tube MSCs) coinjected subcutaneously with tumor cells leaded to tumor progression while hftMSCs administrated intraperitoneally leaded to tumor regression [21]. AT-MSCs promote cancer by secreting galectin-3, but senescent AT-MSCs inhibit. Secretion of IL-6 by UC-MSCs promote also cancer, but when pretreated with IL-6, they gain anti-tumor properties. Senescent BM-MSCs trigger senescent phenotype in proliferating MSCs [22]. There is also evidence that MSCs when attracted to tumor sites can shift their phenotype into an aberrant one that supports tumorigenesis or in rare cases, even fuse with tumor cells, promoting tumor progression [23].

All these aspects show that MSCs can have many variable responses due to many factors, but that effectively they can become great tools in fighting cancer. Unfortunately, there is still a higher number of studies demonstrating that MSCs do have oncogenic effects in the presence of cancer. However, engineered MSCs could eliminate this consequence, by denning or disrupting tumor promoting pathways, or by release of anti-cancer agents with a highest effect than the possible stimulatory effect of MSCs in cancer.

1.2. Cell therapy using engineered MSCs

As mentioned before, engineered MSCs could overcome most of the issues of the negative inherent properties of these cells and effectively make them drug delivery tools to treat for example cancer or to be used in tissue engineering and regenerative medicine.

The majority of MSC dies after a few hours of transplantation, thus engineered MSCs have been made to overexpress pro-survival, pro-angiogenic, or anti-apoptotic genes like protein kinase B (Akt1), adrenomedullin, B-cell lymphoma-2 (Bcl-2), heme oxygenase-1 (HO-1), and others for higher survivability. Another focus in engineered MSCs, is the enhancement of MSC`s migration to injury, inflammation or cancer sites. This can be done with overexpression of homing receptors, such as chemokine receptor 4 (CXCR4) and C-C chemokine receptor type-1 (CCR-1) [24].

In cancer fight, MSCs can be engineered to overexpress therapeutic proteins like interleukins IL-2, IL-12, IL-18, interferon-β, tumor necrosis factor-related apoptosis-inducing ligand (TRAIL) and others. Another approach used is for them to express prodrug-activating enzymes that together with administration of the inactive prodrug locally, became an active drug, killing only the cells in MSCs surroundings, that due to the MSCs tropism, would be cancer cells [24].

Since genetic engineering can only deliver protein drugs, nanoparticles coupled with MSCs (NP-loaded MSCs) have also been used to deliver non-peptidic drugs and therapeutic nucleic acids to target sites. Coupling can be done through cellular internalization or cell surface anchorage, with polymeric or liposomal nanoparticles and release is mostly done through exocytosis and simple diffusion [24].

In the work of Kalimuthu, and colleagues, MSCs were engineered to have an inducible suicide gene for anaplastic thyroid cancer (ATC) eradication. Mouse BM-MSCs were transfected with the designed Tet-On system using a retroviral vector expressing herpes simplex virus thymidine kinase (HSV1-sr39TK). This suicide gene converts the drug ganciclovir (GCV) into cytotoxic GCV-triphosphate and was constructed to be regulated by Doxycycline (DOX). When the engineered cells were cocultured with ATC cells and the prodrug GCV was added and stimulated with DOX, therapeutic gene expression in therapeutic cells and cytotoxicity on target cancer cells was observed [25].

Kari Pollock and colleagues have engineered MSCs to prevent Huntington's disease (HD), a fatal degenerative disease. Human BM-MSCs were engineered using lentivirus in order to secrete high levels of Brain-derived neurotrophic factor (BDNF). This factor is known to prevent cell death and stimulate growth and migration of new neurons in the brain. The test was made in immune-suppressed HD transgenic mice and the result was the increase of neurogenesis and decreased striatal atrophy [26].

1.3. Cancer

Throughout the years, cancer has become one of the most studied diseases duo to the high range of people affected and related mortality. Cancer is a disease caused by a series of alterations in genome and epigenome that lead to activation of oncogenes or inactivation of cancer suppressor genes, thus leading to abnormal proliferation of cells. From all types of cancer, 90% are epithelial, also named, carcinomas and 8% are from leukemias and lymphomas, malignancies in blood and immune cells respectively [27].

Tumors can be divided in two classes according to their spreading risk. A benign tumor doesn't invade surrounding tissue nor migrate to other regions, while a malignant tumor, invades surrounding tissue and can migrate through circulatory and lymphatic systems forming metastases. It is due to their capability of spreading throughout the body that makes malignant tumors such a big challenge to treat [27]. Besides their spreading capability, cancers cells differ in space and time, having intratumor genetic heterogeneity, leading to acquisition of drug resistances *de novo* or by pre-existing resistant subclones, that due to their low number, are not detectable.

In this context, gene and cell-based therapies are emerging as a promising strategy to tackle cancer more effectively, while minimizing the need of surgery and radiotherapy. Since CRISPR-Cas9 seems to be the genome editing tool with higher potential, several attempts are being made in using CRISPR to correct mutated genes or edit cells to use in cell-based therapies [28].

1.4. CRISPR-Cas9

In the last decade, CRISPR-Cas9 system (Clustered Regularly Interspaced Short Palindromic Repeats) has emerged as a programmable tool for site-specific gene editing for prokaryotes and eukaryotes that due to lower price, easier application and higher efficiency [29], has become the favorite nuclease dependent system for gene editing, when compared with TALEN (Transcription activator-like effector nuclease) and ZFN (Zinc finger nuclease).

TALEN is an efficient tool, but two TALENs are always needed in the process. The construction of libraries and multiplexing are technically challenging, just like transformation, due to the large size proteins. Although it is affordable, it is time consuming and protein–DNA interaction is less predictable. Just like TALENs, ZFNs present the same disadvantages, plus a higher price and low reproducibility [30].

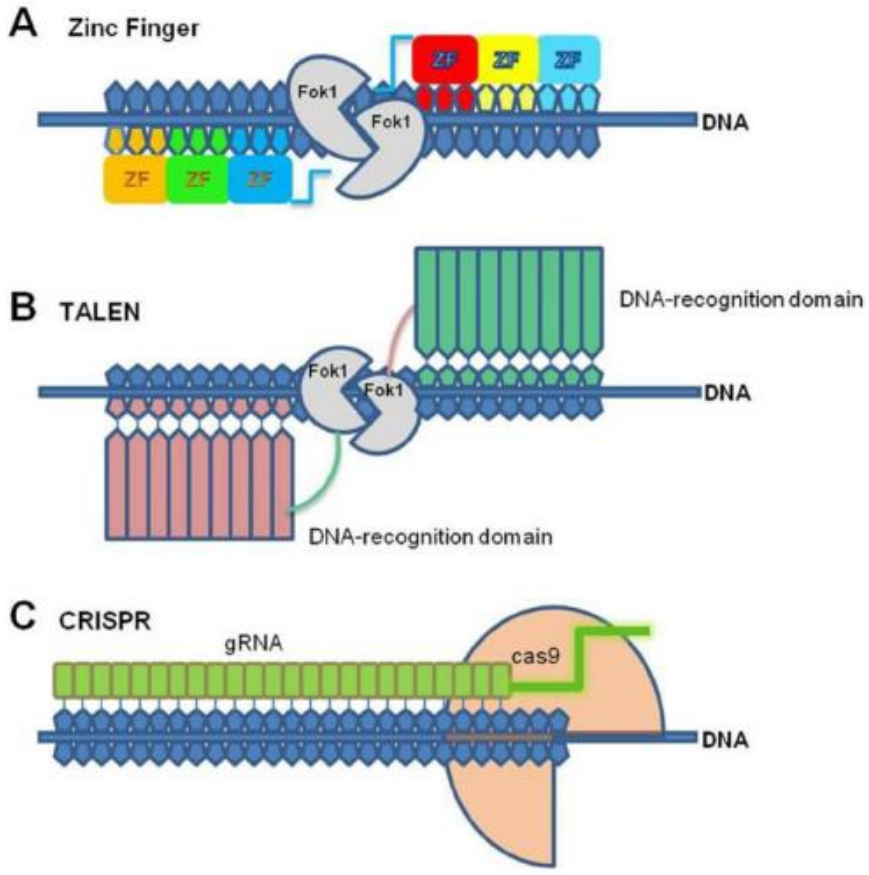

Figure 1: Schematic representation of Genome Editing Tools. **A:** Zinc Finger, **B:** TALEN, **C:** CRISPR-Cas9 [31].

Alteration of gene expression by RNAi also has disadvantages. Since it is a cDNA-based expression system, it can lead to supraphysiological levels of gene expression that can provoke aberrant or artefactual effects on signaling pathways and cell biological processes. Furthermore, gene expression silencing with this tool is limited by gene silencing level and RNAi stability, therefore not being the most proper tool for permanent gene inactivation. Another disadvantage of this tool is the occasional off-target

in case of partial homologies, inherent to the RNA nature of the tool [32]. CRISPR-Cas9 is easily engineered, reproducible and affordable. Unlike the other two mentioned editing systems that need a new engineering protein for every single target, CRISPR-Cas9 only needs a sgRNA (single guide ribonucleic acid) sequence of 20 nucleotides. The DNA–RNA interactions are highly predictable, and construction is highly feasible and affordable [31].

CRISPR-Cas9 system consists in a complex composed of a ribonucleoprotein nuclease Cas9 (the most used is originally from type II CRISPR system of *Streptococcus pyogenes* - SpCas9), which is the element that enhances the cut of the DNA, and a synthetic single guide RNA sequence, containing both CRISPR RNA (crRNA) and trans-activating crRNA (tracrRNA) components , that is bonded to Cas9 and connects to its complementary DNA target sequence in order for the Cas9 perform the cut in the specific site. The sgRNA of 20 nucleotides binds in its 5′-end to the target DNA sequence site while its conserved 3′-end scaffold binds to Cas9 due to the presence of a stem-loop structure in this end, thus making possible the targeting. The Cas9 itself also needs to bind to the DNA, and for that to happen, a PAM (protospacer-adjacent motif) sequence has to be present downstream of the target site. PAM sequence (5′-NGG-3′ in case of SpyCas9), highly occurs in genomes, thus, CRISPR-Cas9 can targeted virtually any gene. Firstly, Cas9 binds to the sgRNA. Secondly, it searches for a functional PAM sequence, dissociating rapidly from mutated PAMs. Once bound to an effective PAM, Cas9 induces the melting of the PAM-adjacent nucleation site by RNA strand invasion to form an RNA–DNA hybrid and a displaced DNA strand (R-loop) from PAM-proximal to PAM-distal ends. If the complementarity is 100%, between sgRNA and target DNA, Cas9 will cut the targeted DNA. The same can happen with high complementary, lower then 100%, thus the possibility of mistargets. To recognize and cut the two strands of DNA substrates, the nuclease domains, HNH and RuvC are needed [33]. The cleavage of the DNA creates a double strand break (DSB) that is naturally repaired by the cell in two possible ways. Usually it is repaired by error-prone non-homologous end joining (NHEJ) pathway, which introduces a small insertion or deletion (InDel) at the site, thus knocking out the gene. The other pathway of repair, called homology-directed repair (HDR), uses, if existent or added, a donor DNA fragment with homology to the flanking sequence that is integrated into the genome at the DSB site, thus repairing the broken DNA [34].

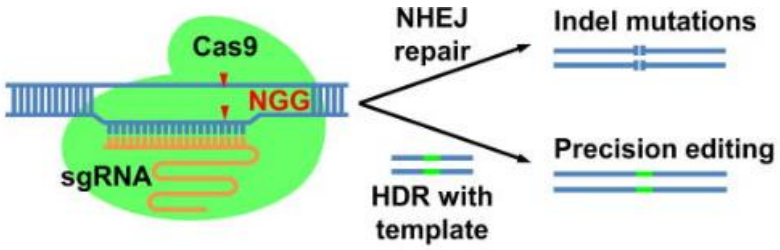

Figure 2: Schematic representation of CRISPR-Cas9 system and double strand break reparation pathways [35].

CRISPR-Cas9 system has improved over the years and changes have been already applied in this system to achieve different varieties and functions of the tool. One example of that is the use of Cas9 nickase (Cas9n), which consists of one inactivating mutation in D10A or H840A to have only one functional endonuclease cleavage domain to generate instead of DSB, single-strand nicks that is prone to be repaired by the high-fidelity base excision repair pathway, using two Cas9n, each associated with sgRNA, one complementary to the 5`strand and the other for the 3`strand of the target site. With this method, off target DSB chances decreases drastically since it is needed two complexes are necessary to target the same location in order to effectively make a DSB [36].

Another alteration of Cas9 is the known dead Cas9 (dCas9) that is generated by double mutations of RuvC and HNH domains in the Cas9 nuclease, thus making the Cas9 incapable of cutting at all but remaining with the specific binding to a target gene region with the right sgRNA. If it targets a promoter of a given gene, dCas9 complex can perturb the gene expression without modifying the DNA sequence through blocking the transcription initiation and elongation. This dCas9 can further suffer alteration with the fusion of transcriptional repressors or activators, hence higher repression or enhancement can also be achieved [36].

One of the limitations of CRISPR-Cas9 system is the efficiency of integration in the living cells and possible cell viability loss. In order to realize permanent Cas9-mediated modifications in cells, introduction of the complex (Cas9 + sgRNA) inside the cell is needed. This can be achieved by introducing plasmids capable of expressing Cas9 and sgRNA genes in the transformed/transfected cells or by transfecting directly transcripts or the ribonucleoprotein (RNPs) complex previously build *in vitro*. In the case of plasmids, two can be used, one expressing the nuclease and the other sgRNA, or an all-in-one plasmid, capable of expressing both. The transformation can be achieved with electroporation, lipofection, polymeric nanoparticles, cell-penetrating peptides or virus like retroviruses and lentiviruses, but disruption of the cell membrane is an aggressive procedure that results in many cell´s casualties, liposomes and virus are limited by efficiency and size and *in vitro* complexes can be toxic to the cells duo to the exogenous nature [37].

Depending on the model and objective, the approach to edit the genome can shift, but the highest nuclease activity is achieved with RNPs and stable expression in cultured cells. However, RNP approach is reliable not only in cells, but also in embryos and *in vitro* assays, being most convenient and functional since is synthesis is not dependent of expression by the cells to be edited. Also, it is the best method to avoid off-targeting due to the shorter exposure to the genome [38].

It is possible to conclude that the targeting of the complex is dependent of many factors such as RNP, plasmid or transcript concentrations, transfection method, target and cell type. In the case of cell types, different percentages of targeting have been seen, even inside the human cell domain, for example, in the work of Mali and colleagues, where targeting rates were compared, and the results showed 10 to 25% of targeting in 293T cells, 8 to 13% in K562 cells, and 2 to 4% in induced pluripotent stem cells. The

target region was AAVS1 locus located in the PPP1R12C gene on chromosome 19, a well-known safe harbor and Cas9 expressing plasmids and transcripts for gRNA were used [39].

Genomic safe harbors (GSHs) are genomic sites in which integration of new genetic material doesn't affect function predictably and doesn't cause alterations in the host that pose any risk in their survival. The AAVS1 site on chromosome 19 previously mentioned, has gained popularity since it is easier to target with the current editing tools and because it can support transgene expression in multiple cell types. Unfortunately, it fails in some cell types and insertions can be silenced by methylation. Also, edition in this site disrupts the PPP1R12C gene (phosphatase 1 regulatory subunit 12C) [40].

Unfortunately, the effective edition of cells' genome using Cas9 RNP, even though, higher than using plasmids, is very low, as it has been showed in the work of Brock Roberts and Amanda Haupt, in which the repaired human induced pluripotent stem cells (hiPSC) with HDR were <0.5-4%. However, most of the resultant cells developed good morphology, stable genome and gene expression and right location of the edition product [41].

In order to produce a CRISPR-Cas9 RNP complex *in vitro*, *E. coli* can be used to produce Cas9 protein with the right expression plasmid, and gRNAs can be constructed and amplified. Carolin Anders and Martin Jinek of Department of Biochemistry of University of Zurich were able to produce and purify Cas9 protein, using *E. coli* strain Rosetta 2 DE3. Cells are lysed in cell homogenizer and Cas9 is purified with consecutive techniques of chromatography and concentrations, more precisely IMAC, Dialysis and 6His-MBP cleavage, IEX and SEC [42].

Since the CRISPR-Cas9 is capable of targeting and cutting pre-determined genetic sequences, it is expected that it would be used in gene therapy for example, for disruption of proliferative genes in cancer cells, genes for viral proteins, mutated genes that provoke genetic diseases or even being used with donor vectors for effective repair [43].

1.5. Gene and Cell therapy using CRISPR-Cas9 for anti-cancer therapies

Biotechnology, together with medicine, has developed over the last decades therapies using gene edition and cell transplantation or transfusion in order to regenerate and cure diseases that in the past would require radiotherapy, chemotherapy and/or surgery, procedures with high risk and heavy consequences. With the discovery of tools to edit DNA, researchers began editing and alter the cells genome for transplantation, to enhance results and create new approaches. Unfortunately, most of these therapies are currently experimental since it is a recent born field with still a lot of gaps of information and knowledge and high risks if not performed correctly [44].

Genes define the structure and machinery of the organisms and that includes the human being. In case of mutations, genetic diseases are born, and these can be inherited or developed in response to environmental stresses such as viruses or toxins. In all diseases it is possible to correlate to a genetic background, even in those that are not genetic diseases. With a continued growing knowledge of the genetic mechanisms responsible for the diseases, more and more early diagnostics are possible, new treatments emerge and new ways of prevention appear, especially with the recent development of tools like CRISPR-Cas9 that can edit specifically pre-determined genes. [44] The therapies aimed to cure genetic diseases are more likely to be based in gene therapy in which the genome is edited *in vivo* permanently. Another concept used more often in regenerative medicine and in cancer and other genetic diseases treatment is cell therapies.

Engineered cells can be used not only as regenerative tools but also as vectors since some cells have defined tropism and hence, they can be engineered to secrete determined factors to specific tissues. Cell therapies are classified by the targeted disease, the origin and type of cells in use. Nowadays, cell therapies have been developed to target all types of diseases including cancer, Parkinson's disease, Amyotrophic lateral sclerosis, Alzheimer, Stroke, Spinal Cord Injury, Multiple Sclerosis, Radiation Induced Intestinal Injury, Inflammatory Bowel Disease, Liver Disease, Duchenne Muscular Dystrophy, Diabetes, Heart Disease, Bone Disease, Renal Disease, Chronic Wounds, Graft-Versus-Host Disease, Sepsis, Respiratory diseases, etc. [45].

For each therapy, defined by the type of tissue damaged, different progenitor cells can be used. For example, neural stem cells are used in regeneration in brain damage cases, while hematopoietic stem cells are focused on blood diseases such as leukemia. Another important issue is the origin of those cells. These have to be compatible so that immune responses can be avoided, and engraftment can be achieved. Transplant can be autologous if the cells, grown normally in ex vivo, were originally from the patient. The transplant is allogenic if the cells came from a donor [46].

The EU regulatory classification of cell therapies discriminates between minimally manipulated cells for homologous use (transplants or transfusions) and those regulated as medicines which are required to demonstrate quality, safety and efficacy standards to obtain a marketing authorization before becoming commercially available (referred to as Advanced Therapy Medicinal Products; ATMPs). These are further subdivided into somatic cell, gene therapy and tissue engineered products [46].

All of these therapies involve genetic engineering and therefore it is normal that most of them will be based on the use of CRISPR-Cas9, the best tool for such purpose. The following table describes the many research treatments in the most relevant diseases, using CRISPR-Cas9 system for gene therapy:

Table 1: Summary of most revolutionary gene therapies using CRISPR-Cas9 system.

Type	Disease	Target genes	CRISPR-Cas9 integration	model	Reference
Genetic diseases	Duchenne muscular dystrophy (DMD)	*Dmd (exons 51, 44, 45, 53)*	Adeno-associated virus (AAV)	myofibers, cardiomyocytes, muscle stem cells *in vitro,* mice zygote	47--50
	Cystic fibrosis	*CFTR (exon 10,11, intron 11, 12, 19, 22)*	CRISPR-Cas9 and transposase mediated excision in plasmid	HEK293T cells, intestinal stem cell organoids	51--53
	Leuckemia	*BCR/ABL fusion, IDH2 R140Q*	Lentivirus	Boff-p210, xenograft model of CML	54--55
	Hearing loss DFNA36	*Tmc1*	n.d.	mice model	56
	Retinal disease	*RPE65, CEP290, Nrl, S334ter,P23H, Mertk, VEGF-A, VEGF-R2, Mgat5*	Adeno-associated virus (AAV)	LCA 2 mouse model,autosomal dominant retinitis pigmentosa mouse model, Ipsc	57--62
	Alzheimer's disease (AD)	*PSEN2*	Plasmids	human BFCNs from iPSCs with PSEN2 mutation	63
Viral infection	Human Papillomaviruses (HPVs)	*E6, E7*	Adeno-associated virus (AAV), plasmids	HeLa, 293T and SiHa cells with HPV	64--66
	Hepatitis B virus (HBV)	*HBV core, surface proteins*	Plasmids	Huh7 cells, hydrodynamics-HBV persistence mouse model, cell line A64	67--73
	Epstein-Barr virus (EBV)	*EBNA1, EBNA3C, LMP-1, BART*	Plasmids	Burkitt's lymphoma cell line with latent EBV strain B95-8 infection	74--77
	HIV-1 virus	*LTR4, LTRB, MA3, PR1-PR5, RT2-RT4, RT6,IN1, IN2, IN4, IN5, IN7, NF-kB binding site,TAR*	Lentivirus, Adeno-associated virus (AAV)	T cells, Tg26 mice, acutely infected mice, humanized bone marrow/liver/thymus (BLT) mice, SupT1 cells	78--83
Cancer	Lung cancer	*PD-1 EGFR T790M, KRAS G12D*	Lentivirus	Injection of editted immune cells of patient, small cell lung cancer	84--86
	Prostate cancer	*AR, GPRC6A (exon 3), HNRNPL*	Lentivirus, aptamer-liposome-CRISPR/Cas9 chimera, adenovirus	LNCaP cells, PC-3 cells, hepatocellular carcinoma cells *in vitro*, mouse xenografts	87--90
	Breast cancer	*CDH1, PTEN, p53, BRCA1, BRCA2, HER2 exons*	CRISPR-dCas9 epigenetic editing tool,	breast cancer cell *in vitro*	91--94
	Thyroid cancer	*TWIST2, NOX4, NADPH oxidase, BRAF-V600E*	*in vitro* assemble, plasmid	HeLa cells, HEK293T, A375 cell lines	95--96
	Bladder cancer	*HRAS, hUP II, hBAX, p21, CDH1*	lentivirus, plasmids, CRISPR-Cas-aptamer	bladder cancer cells T24 and 5637, J82, 5637 and SW-780 cells	97--99
	Pancreatic cancer	*Frizzled-5, KRAS2, CNKD2A, TP53, SMAD4*	lentivirus	nude mice	100

Among many diseases, genetic disorders are a great target for gene therapy, and many advances have been made in order to treat them, with higher incidence in the most mortal and predominant diseases. Most of the treatments are based in gene knockout and homology direct repair using the correct gene template, using transfected plasmids or virus. The following examples of treatments have as objective showing the diversity of possible targets of CRISPR-Cas9 treatment and the variety of methods and logistic used.

Chronic myeloid leukemia (CML) is a malignant myeloproliferative disorder provoked by hematopoietic stem cells that acquire a reciprocal translocation between the long arms of chromosomes 9 and 22 generating the BCR-ABL oncogenic fusion protein that transforms the hematopoietic progenitor cells by activating downstream signaling proteins that increase cell survival and proliferation.

A possible treatment is CRISPR-Cas9 ablation of BCR/ABL fusion gene. This was tested *in vitro* (Boff-p210 is a murine interleukin 3 (IL3)-independent cell line derived from the hematopoietic cell line Baf/3

that expresses BCR/ABL as a tetracycline regulated transgene) and in the *in vivo* xenograft model of CML, with lentiviral constructs for sgRNAs targeting the gene fusion, and others for Cas9 constitutive expression. The result was positive, with highly effectiveness at inducing indels in their target sequences [54].

Among all cancer types known to man, lung cancer is the deadliest, being the main cause of cancer-related deaths, and the second most common cancer type, affecting 1.8 million people. Chemotherapy has showed incapability to efficiently treat lung cancer, even though it can improve the patient's condition. [82] The first injection of edited cells with CRISPR-Cas9, in humans, was performed in clinical trials for lung cancer treatment in China 2016. Immune cells of the patient`s blood were removed and edited with CRISPR–Cas9 to disable the gene encoding PD-1, a protein that suppresses extreme immune responses. After culturing the edited cells to reach an acceptable number, cells were injected back to the patient with metastatic non-small-cell lung cancer. Since there is no brake in immune response, it is expected a bigger attack to the cancer cells and possibly complete eradication [86].

Another concept created to fight the resistance acquisition from cancers is a high complex CRISPR-barcoding system capable of detecting thousands of distinct sequences by qPCR or deep-sequencing, therefore being capable of tracking single cancer cells including the rare pre-existing resistant subclones that might plant the seeds for drug resistance. This system was develop for models of drug resistance in non-small cell lung cancer (NSCLC), more precisely for NSCLC resistant to EGFR inhibitors based on a specific sgRNA and a donor single stranded DNA oligonucleotide (ssODN) containing as barcodes different genetic aberrations, including the EGFR T790M mutation, a secondary mutation in the catalytic domain associated to acquired resistance and KRAS G12D mutation, a well-known negative predictor for primary responsiveness to EGFR inhibitors [84].

Prostate cancer has the highest occurrence in the world and is the second cancer that takes more men`s lives in United States. A possible treatment with CRISPR-Cas9 for such cancer is targeting the gene that express the androgen receptors (AR), therefore, stopping the binding of androgens like male hormones that stimulate cell proliferation. Since the androgens are the primary responsible for prostate cancer, suppressing their action would be a good option of treatment. For such effect, sgRNAs were designed to target three different regions of the AR gene and tested in androgen-positive prostate cancer cell lines *in vitro*. Lentiviral vectors (LVs) with the genes for Cas9 and sgRNA were transfected in LNCaP cells, androgen-sensitive human prostate adenocarcinoma cells derived from the left supraclavicular lymph node metastasis. The result of such test was positive, with effective disruption of the Ars that leads to apoptosis and consequently inhibition of the growth of the androgen-sensitive prostate cancer cells. [87] The gene knockout treatment has potential and new targets are being searched, such as the heterogeneous nuclear ribonucleoprotein L (HNRNPL), a ribonucleoprotein (RNP) that regulates the alternative splicing of RNAs, including the ones that encode the androgen receptors, the principle enhancer of the prostate cancer [88].

A different approach was also designed to kill prostate cancer cells using a flexible aptamer-liposome-CRISPR/Cas9 chimera to target prostate cancer cells and their survival gene, polo-like kinase 1.

One issue in using CRISPR-Cas9 to target specific cells is the delivery into target cells, so using an RNA aptamer that specifically binds to prostate cancer cells expressing the prostate specific membrane antigen, and that is linked to a cationic liposome with CRISPR-Cas9, would drastically increase the efficiency of delivery and therefore efficacy of the therapy. The result of the use of such chimera in LNCap and PC-3 cells was silencing of the prostate cancer *in vivo*. [89] CRISPR-Cas9 has been also used for insertion of suicide genes in the prostate cancer cells, for tumor decrease and potential elimination [90].

Until now, most of the therapies refereed previously belong to the field of gene therapy, but CRISPR-Cas9 system can also be used to edit cell *ex vivo,* for further culture and transplantation or transfusion, being this method part of the field of cell therapy.

One recent study used CRISPR-Cas9 to engineer chimeric antigen receptor (CAR) T cells universal, potent and resistant to exhaustion, for immunotherapy. These T cells have been altered to acquire tumor-targeting receptors for treating various leukemias and lymphomas and may eventually be used to treat solid cancers. They have extracellular single-chain variable fragment (ScFv) specific to an antigen on tumor cells and an intracellular chimeric signaling domain for T cell activation and tumor killing. To became universal, T cells genome was edited to make these cells deficient in the expression of endogenous T cell receptor (TCR) and HLA class I (HLA-I). Genome editing have been further used to enhance their function by disrupting genes of inhibitory receptors or signaling molecules, such as programmed cell death protein 1 (PD1) or cytotoxic T lymphocyte-associated protein 4 (CTLA4). This system has been already tested to target CD19, an antigen expressed by B cells and B cell malignancies and Her2/neu, Mesothelin cMet, GD2, interleukin-13 receptor alpha 2 (IL13Rα2), CEA, and EGFR, for targeting solid tumors treatment [101]. Another negative regulator of T cell activity is lymphocyte activation gene-3 (LAG-3), that has also been knockout in CAR-T cells for high efficiency using CRISPR-Cas9 system, with viability and immune phenotype almost unchanged during in vitro culture [102].

SMART cells (Stem cells Modified for Autonomous Regenerative Therapy), were develop into cartilage cells that produce biologic anti-inflammatory drugs, such as TNF-α or IL-1 inhibitors (TNF-α and IL-1 are responsible for inflammation). It is an innovational way to deliver the drugs only in the joints, losing the need for systemically administration. The new cartilage cells will replace arthritic cartilage, and protect against chronic inflammation, preserving joints and other tissues. These engineered cells were achieved with CRISPR-Cas9 genomic edition. This concept can be used to many other disease treatments, since it uses the cells basically as producers and delivers of drugs [103, 104].

1.6. Azurin

Azurin is a blue copper protein of redox nature with a molecular mass of 14 kDa founded in *Pseudomonas aeruginosa* and involved in the bacterial denitrification. [105] Besides azurin's role in *P. aeruginosa*, this protein can interact with molecular pathways of tumor cells, leading to apoptosis of the targeted cancer cells. Capable of entering in the cell´s nucleus, azurin stabilizes p53, increasing is activity and release of cytochrome c into the cytosol, activating caspase cascade that leads to cellular apoptosis. [106] Not only has natural cytotoxicity to cancer, it also shows preferential entry into cancer cells, thus showing potential as tool against cancer [107].

Azurin is known to reduce metastization of tumor tissue by interfering with overexpression of cell-cell adhesion molecules like P-cadherin in cancer cells, thus reducing the capability of migration of the tumor cells. It also inhibits VEGFR-2, decreasing hyper-phosphorylation levels of FAK and Src non-receptor tyrosine kinases correlated with intracellular changes in the cytoskeleton and cell-cell adhesion proteins that decreases migration [108, 109]. Being an antagonist of ligand ephrinB2, it also binds to the extracellular EphB2 tyrosine kinase receptor, thereby inhibiting cancer cell´s growth [110].

For all previous mentioned reasons, azurin would make a great anti-cancer drug and if expressed by cells with tropism for cancer, could became an efficient treatment against cancer.

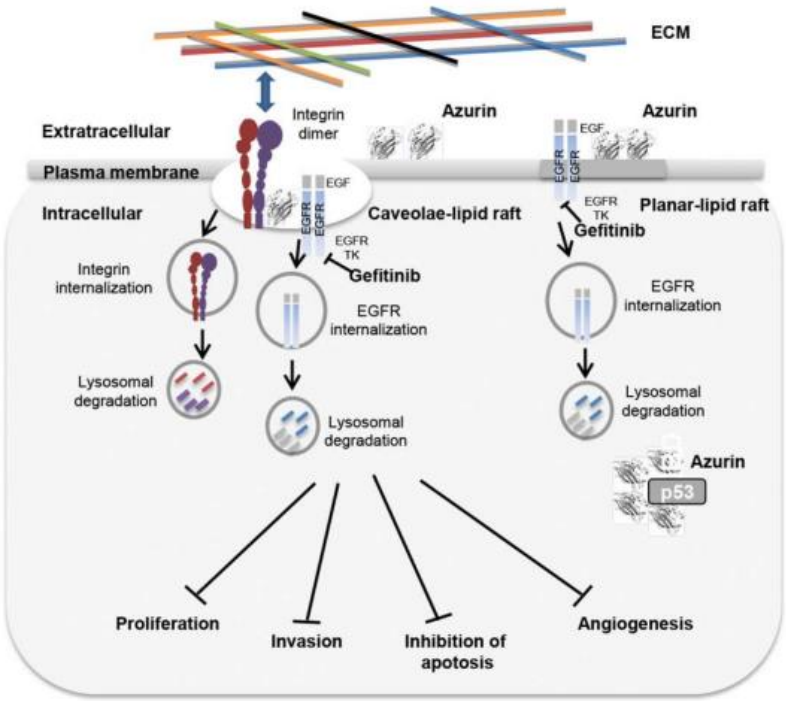

Figure 3: Mechanisms of azurin. Gefitinib binds to the intracellular enzyme (tyrosine kinase) of the EGFR ultimately inducing anti-proliferative effects. Azurin binds to cancer cells through binding to lipid raft components and cell-surface receptors. Upon entry, azurin interferes in cancer cell growth by multiple mechanisms including complex formation with p53.

In this study, we aim to produce and purify Cas9 protein to edit MSCs genome efficiently with an RNP transfection approach and test efficiency of cleavage in HEK, HeLa and MSC cells *in vitro* and in HEK cultured cells for future integration of an azurin template in order for these engineered cells to become an anti-cancer cell therapy due to tumor cells tropism of the MSCs.

2. Study's objective and strategy

This study is part of an ongoing project of IBB with the final objective of engineering MSCs capable of migrate *in vivo* to the tumor locations and produce and secrete azurin, a bacterial protein with anti-cancer properties that is expected to be non-toxic for normal cells, thus creating a new cell therapy against cancer. Using the natural tropism of MSCs to tumor cells, these cells can be used as drug delivery vehicles. By integrating permanently, the azurin coding-sequence in the cells genome, the changes will pass through cell division to the new cells, thus producing an immortal culture of MSCs capable of expressing and secrete azurin. The edition will be made using CRISPR-Cas9 system in order for permanent integration of the azurin expression in these cells. The migratory capacity of BM-MSCs *in vitro* towards cancer cells was tested as well as azurin influence in MSCs proliferation and entry capacity. An azurin recombinant plasmid called pVAX-Azurin was constructed for BM-MSCs microporation and identification of azurin expression and tumor growth inhibition upon treatment with azurin-MSC conditioned medium. A gRNA sequence targeting the AAVS1 genome safe harbor was already tested in HEK293T cells with the all-in-one plasmid strategy. The first aim of this thesis is to test the best conditions to transfect MSC cells by electroporation with the same plasmid. Furthermore, another aim of this study is the overexpression in *E. coli* system and purification of Cas9 protein in order to construct *in vitro* the CRISPR-Cas9 RNP complex for further transfection in MSCs. *In vitro* cleavage assays will be tested in HEK, HeLa and MSCs. The efficiency tests will also be performed in HEK to observe cleavage efficiency of the complex.

3. Materials and Methods

3.1. Transformation of *E. coli BL21(DE3)*

E. coli DH5α cells containing the plasmid pMJ923 (Addgene plasmid # 78313, a kind gift from Martin Jinek) were grown overnight in LB medium containing ampicillin (1 µg/mL), at 37 ºC and constant agitation of 250 rpm. For plasmid extraction, NZYMiniprep kit (NZYTech) was used, following the manufacturer's instructions. After extraction, purified plasmid DNA concentration was determined with Nanodrop™ (ND-1000 Spectrophotometer). 10 ng of plasmid were used to transform competent *E. coli* BL21 (DE3) by electroporation (25 µFD capacitance, 400 Ω resistance, 2.5 kV; Gene Pulser™, Biorad). After the shock, cells recovered in LB medium for 1h at 37 ºC with constant agitation of 250 rpm and were plated in LB agar plates containing ampicillin (150 µg/mL).

3.2. Cell Culture and Overexpression of Cas9

Transformed *E. coli BL21(DE3)* was cultured in SB medium with ampicillin (150 µg/mL) at 37 ºC with constant agitation of 250 rpm until it reaches exponential phase (OD between 0.6-0.8). Samples were taken at this point for SDS-PAGE and Western blot analysis (Time zero samples). IPTG (Isopropyl-β-D-thiogalactopyranoside) was added at a final concentration of 0.2 mM for the induction of Cas9 expression and incubated at 25 ºC with constant agitation of 250 rpm, for 5-6h. Samples were taken at the end of this time for SDS-PAGE analysis and Western blot.

Cells were centrifuged at 4º C, 8000 rpm for 10 min (Beckman J2-MC Centrifuge) and the pellet was resuspended in Binding/Start buffer (20 mM Tris-Cl, pH 8.0, 250 mM NaCl, 10 mM imidazole, pH 8.0) and conserved at -80 ºC. 8% SDS gels and Western blots were made to visualize Cas9 expression. The same was applied for each step of purification.

3.3. SDS-PAGE and Western bolt

The polyacrylamide gels were made with a resolving layer of 8% or 12% and a stacking layer of 5%. Samples of cell or protein suspensions were lysed or denatured, respectively, with loading buffer (Tris 1M pH 6.8, SDS 2.0%, glycerol 10%, bromophenol blue 0,0006%, DTT 0.1M) in a dry bath at 95-100 ºC for 5 min in order to run in electrophoresis. In bacterial cell lysates, a centrifugation at 9000 rpm for 1 min. was also made to remove debris. SDS-PAGE was run with Electrophoresis Buffer 1X for 10 min at 75 V and 120 V until the end of migration. BlueSafe or Comassie was used to dye the gel in order to observe the protein´s migration. To continue Western blot procedure, transfer of the proteins of the gel to a membrane of nitrocellulose was done using TransBlot Turbo and Transfer Buffer 1X at 15 V for 15 min. Ponceau 4R

was used to confirm correct transfer. Blockage of the membrane was made with non-fat dry milk 5% (w/v) in PBS Tween for 1h with smooth agitation, followed by incubation overnight at 4º C with smooth agitation with anti-His anti-bodies (His-probe (H-3) sc-8036 mouse monoclonal IgG_1 from Santa Cruz Biotechnology) diluted 1:1000 (v/v) in the milk solution. Membrane was washed with PBS Tween for posterior incubation with secondary antibodies coupled with HRP (goat anti-mouse IgG-HRP sc-2005 from Santa Cruz Biotechnology), diluted 1:2000 (v/v) in PBS Tween for 1h. Membrane was washed for posterior addition of ECL reagent and consequent protein detection in Fusion Solo VILBER LOURMAT with exposure between 3 and 10 min.

3.4. Cas9 purification and MBP-6His cleavage

Per purification, 6-8L of cell suspension were resuspended in Binding Buffer for sonication. The parameters used in BRANSON SONIFIER 250 were the following: Duty cycle of 50 % and Output of 10, 9 cycles, 15 pulses each cycle, with intervals of 5-10 min. After the sonication, the lysate was centrifuged at 4 ºC, 17,600xg for 5 min., and the resulting supernatant was centrifuged again in the same conditions for 1h. The supernatant was applied in IMAC column (Immobilized metal affinity chromatography) in which the His tag will bind to the nickel from the column HisTrap™ FF 5 mL (GE Healthcare).

IMAC was performed in AKTA start (GE Healthcare) after washing the system with dH_2O and equilibrated with Binding Buffer A (20 mM Tris-Cl, pH 8.0, 250 mM NaCl, 10 mM imidazole, pH 8.0). After multiple sample applications and washouts to avoid column clogging, the protein was eluted with Elution Buffer B (20 mM Tris-Cl, pH 8.0, 250 mM NaCl, 250 mM imidazole) in a linear gradient from 0-100% of Elution Buffer.

Table 2: Parameters of IMAC program for Cas9 purification.

Column volume	5.027 mL
Pressure limit	0.30 MPa
Flow rate	5 mL/min.
Equilibrium with	1 CV
Sample volume	~20 mL
Wash column with	6 CV
Elution type	Gradient
Start %B	0.0 %
Set target concentration	100% B
Gradient volume	20 mL
Equilibrate with	5 CV

Protein purity along the purification was analyzed with 8% SDS-PAGE gels. The fractions containing higher levels of the target protein were concentrated with Amicon Ultra Centrifugal (Milipore),

with a molecular weight cut-off of 10,000 Da, at 4000 rpm, 4 ºC (Epp. Centrifuge) with a final volume of 3 mL.

Imidazole was removed by dialysis with Dialysis Buffer (20 mM HEPES-KOH, pH 7.5, 150 mM KCl, 10 % (v/v) glycerol, 1 mM dithiothreitol (DTT), 1 mM EDTA). The Cas9 fusion protein produced has a TEV sequence for MBP-6His cleavage and in order to do both steps together, the purified Cas9 is inserted in a Slide-A-Lyzer™ G2 Dialysis Cassette (ThermoFisher Scientific), 10K MWCO, 3 mL with 1.5 µM of TEV and left with smooth agitation at 4 ºC. Dialysis was extended for 2-3 days for higher cleavage efficiency.

After dialysis, Cas9 was further purified by IEX using HiTrap™ 5 mL SF HP (GE Healthcare) that was first washed with dH_2O and IEX Buffer A (20 mM HEPES-KOH, pH 7.5, 100 mM KCl), before protein application. Elution is performed with a linear gradient of IEX Buffer B (20 mM HEPES-KOH, pH 7.5, 1 M KCl) form 0-50%. Fractions containing Cas9 were pooled and concentrated with Amicon Ultra Centrifugal (Milipore), with a molecular weight cut-off of 50,000 Da, at 4000 rpm and 4 ºC until a final volume of 500 µL.

Table 3: Parameters of IEX program for Cas9 purification.

Column volume	5.027 mL
Pressure limit	0.30 MPa
Flow rate	5 mL/min.
Equilibrium with	2 CV
Sample volume	2 mL
Wash column with	5 CV
Elution type	Gradient
Target %B concentration (0-100%)	50%
Volume 0-100 (CV)	12
Start %B concentration	0%
Equilibrate with	5 CV

The last step for Cas9 purification was SEC (Size Exclusion Chromatography). The column Superdex 200™ 10/300 was previously washed with dH_2O and SEC Buffer (20 mM HEPES-KOH, pH 7.5, 500 mM KCl, 1 mM DTT) and the parameters used in the program are represented in Table 4.

Table 4: Parameters of SEC program for Cas9 purification.

Column volume	24 mL (30 cm x 100 mm)
Pressure limit	1.5 MPa
Flow rate	0.5 mL/min.
Equilibrium with	1 CV
Sample volume	500 µL
Wash column with	5 CV

After SEC, concentration of the enriched fractions was made with Milipore 50,000 MWCO Amicon and Cas9 quantification was made with spectrophotometer at 280 nm and an extinction coefficient of 120,450 M^{-1} cm^{-1}, according to C. Anders and M. Jinek [42]. The resultant Purified Cas9-mCherry protein was divided into 300 µL aliquots for further flash freeze with liquid nitrogen and storage at -80 ºC, until is use.

3.5. Cell Culture and Overexpression of TEV

E. coli BL21(DE3) cells were transformed with pRK793 plasmid (Addgene plasmid # 8827) and cultured in SB medium with ampicillin (150 µg/mL) at 37 ºC, 250 rpm until it reaches exponential phase (OD between 0.6-0.8). Samples were taken at this point for SDS-PAGE and Western blot analysis (Time zero samples). IPTG (Isopropyl-β-D-thiogalactopyranoside) was added at a final concentration of 1 mM for TEV expression induction and incubation was made at 30 ºC with constant agitation of 250 rpm, for 4-6h. Samples were taken at the end of incubation for SDS-PAGE analysis and Western blot.

Cells were centrifuged at 4º C, 8000 rpm and for 10 min (Beckman J2-MC Centrifuge) and the pellet was re-suspended in Binding/Start buffer (20 mM Tris-Cl, pH 8.0, 250 mM NaCl, 10 mM imidazole, pH 8.0) and conserved at -80 ºC. 12% SDS gels and Western blots were made to visualize TEV expression. The same was applied for each step of purification.

3.6. TEV purification

2L of cell suspension were re-suspended in Binding Buffer A (50 mM sodium phosphate, pH 8.0, 200 mM NaCl, 10% glycerol, 25 mM imidazole). Sonication was used to lyse the cells, in BRANSON SONIFIER 250 equipment with the following conditions: Duty cycle of 50 % and Output of 10, 9 cycles, 15 pulses each cycle, with intervals of 5-10 min. After sonication, cell lysate was centrifuged at 4 ºC, 17,600xg for 5 min., and the resulting supernatant was once again centrifuged with the same conditions for 1h. The supernatant was applied to an IMAC (Immobilized metal affinity chromatography; column HisTrap™ FF 5 mL, GE Healthcare).

IMAC was performed in AKTA start (GE Healthcare) after washing the system with dH_2O and equilibrated with Binding Buffer A. The protein was eluted with Elution Buffer B (50 mM sodium phosphate, pH 8.0, 200 mM NaCl, 10% glycerol, 250 mM imidazole) in a linear gradient from 0-100% of Elution Buffer.

Table 5: Parameters of IMAC program for TEV purification.

Column volume	5.027 mL
Pressure limit	0.30 MPa
Flow rate	5 mL/min.
Equilibrium with	7 CV
Sample volume	~20 mL
Wash column with	15 CV
Elution type	Gradient
Start %B	0.0 %
Set target concentration	100% B
Gradient volume	20 mL
Equilibrate with	10 CV

Protein purity along the purification was analyzed with 12% SDS-PAGE gels. The fractions containing higher levels of the target protein were concentrated with Amicon Ultra Centrifugal (Milipore), with a molecular weight cut-off of 10,000 Da, at 4000 rpm, 4 ºC (eppendorf S804R Centrifuge) with a final volume of 2 mL. In the pool, EDTA was added to a final concentration of 2 mM and DTT to a final concentration of 5 mM.

Gel filtration was performed in Amersham Biosciences XK16 column of 120 mL. The Gel filtration Buffer used was: 25 mM sodium phosphate (pH 7.5), 100 mM NaCl, 10% glycerol, using the conditions in Table 6.

Table 6: Parameters of Gel filtration program for TEV purification.

Column volume	120.637 mL
Pressure limit	0.15 MPa
Flow rate	0.5 mL/min.
Equilibrium with	0 CV
Sample volume	2 mL
Wash column with	1.5 CV

Enriched fractions of TEV were concentrated with an Amicon Ultra Centrifugal (Milipore), with a molecular weight cut-off of 10,000 Da, at 4000 rpm, 4 ºC. Quantification was made with spectrophotometry at 280 nm and a molar extinction coefficient of 32,290 M^{-1} cm^{-1} according to Joseph E. Tropea and colleagues [112]. The resultant Purified TEV protein was divided into 300 µL aliquots for further flash frozen with liquid nitrogen and stored at -80 ºC until use.

3.7. Microporation of MSCs with All-in-one plasmid

Transfection of MSCs with all-in-one plasmid with Cas9 from *S. pyogenes* with 2A-EGFP (pX458 plasmid Addgene at # 48138) was performed using Neon Transfection System (Thermo Fisher Scientific), according to Madeira *et al*, 2011 [113]. Cells were washed with PBS 1X and detached from plastic surface using TriplE Select. 100 000 cells were resuspended in R Buffer (provided by the manufacturer) and microporated with 0.5 µg of plasmid DNA in a final volume of 10 µL. In this experimented, 24 microporation conditions, varying pulse voltage (mV), pulse width (ms) and pulse number, were tested. After such procedure, cells were immediately transferred to Opti-MEM™ medium (GIBCO™) to increase cell viability after transfection and plated in 24-well-plates previously coated with CELLstartTM and StemPro® MSC SFM XF medium (GIBCO™). 24 hours post-transfection, culture media was replaced, and cells were incubated at 37 ºC with 5% CO_2 for 48 hours.

3.8. Flow cytometry of MSCs

After microporation, cell viability and GFP expression was analyzed with flow cytometry. (FACSCalibur equipment, Becton Dickinson; FL1 filter), where GFP fluorescence intensity was measured after 48h of cell incubation. Cells were washed with PBS 1x, detached using TriplE Select 1x and counted using the trypan blue dye exclusion test. Afterwards, cells were centrifuged in FACS tubes at 1000 rpm for 5 min., fixed in 300 µl of 2% Paraformaldehyde (PFA) in PBS 1x and cells were analyzed within the following hour.

3.9. *In vitro* CRISPR-Cas9 cleavage assay

HEK, HeLa and AT-MSCs (Adipose Tissue-MSCs) were cultured in 6 well-plates for posterior DNA extraction. Medium was removed, and cells were washed with PBS 1X two times. 60 µL of ATL Buffer were added and cell scrapers were used to free lysate. It was added to the lysate 5 µL of RNaseA 100 mg/mL and 20 µL of Qiagen Proteinase K solution. It was Incubated for 2-3h in dry bath at 57 ºC. Next it was vortexed for 15 sec. It was added 200 µL of absolute ethanol and 200 µL of AL Buffer. Vortex was repeated, and solution was transferred to DNeasy Mini Spin with a collection tube of 2 mL. It was centrifugated at 8000 rpm for 1 min., discarding the collection tube and switching for a new one, adding posteriorly 500 µL of AW1 Buffer. It was centrifuged at 8000 rpm for 1 min., discarding the collection tube and switching for a new one for posteriorly adding 500 µL of AW2 Buffer. It was centrifuged at 14 000 rpm for 3 min., discarding the collection tube and switching for a 2 mL Eppendorf and 200 µL of AE Buffer were added. The solution was Incubated at room temperature for 1 min. and centrifuged for 1 min. at 8000 rpm. Quantification was made in Nanodrop for DNA concentration and purity. The DNA resultant from DNA extraction was mixed with Na acetate 3 M for a final concentration of 0.1X and with absolute ethanol for a final concentration of 2.5X. The solution was incubated at -80 ºC for 1h. It was centrifuged for 30 min. at 4 ºC at 15 300 rpm and supernatant was removed. It was added 500 µL of ethanol 70% and resuspension was performed. It was centrifuged for 10 min. at 4 ºC, at 15 300 rpm and supernatant was removed. Speed vacuum for 15 min. at 60 ºC was made and for further resuspension in 20 µL of dH_2O. DNA quantification was once again made using Nanodrop.

Firstly, the double-stranded DNA template as cleavage substrate was generated through PCR amplification of the target region. DNA samples were diluted to 3 ng/µL in RNA-free water. 2 µL of the resultant DNA solution were mixed with 1:1 (Fw/Rev) mix of primers, 25 µL of AmpliTaq Gold ® 360 Master mix to a final volume of 50 µL. The following PCR program was used:

Table 7: PCR program for DNA substrate amplification.

Enzyme activation	15 ºC	10 min.	1X
Denaturation	95 ºC	30 sec.	40X
Anneal	60 ºC	30 sec.	
Extend	72 ºC	30 sec.	
Final Extend	72 ºC	7 min.	1X
Hold	4 ºC	Hold	1X

PCR products were run in a 1.3% Agarose gel at 90 V to assure correct amplification.

The Alt-R CRISPR-Cas9 System (Integrated DNA Technologies) was used to generate synthetic guide RNAs (crRNA and trancrRNA) to test the in *vitro* cleavage efficiency of the *in house* obtained Cas9 protein. Lyophilized RNAs were re-suspended with IDTE Buffer (Tris 10 µM pH 7.5, EDTA 1 mM, not provided) to a final concentration of 100 µM. To generate the RNA duplex (crRNA:trancrRNA; gRNA), both oligos were mixed in equimolar concentrations to a final duplex concentration of 10 µM, and incubated in dry bath at 95 ºC for 5 min. The solution was cooled to room temperature before preparing the RNP complex. Cas9 was added to the gRNA duplex prepared, to a molar ratio of 1:1 inCas9 dilution buffer (30 mM HEPES, 150 mM KCl, pH 7.5). It was further incubated for 10 min at room temperature for RNP formation. Finally, the in vitro digestion reaction was performed by mixing 1µM of RNP, with 100 nM DNA substrate in Cas9 Nuclease Reaction Buffer (200 mM HEPES, 1 M NaCl, 50 mM $MgCl_2$, 1 mM EDTA, pH 6.5 at 25°C), at room temperature followed by 1h incubation at 37 ºC. To release the DNA substrate from the Cas9 protein, 20mg/mL of Proteinase K was added and incubated at 56 ºC, for 15 min. Cleaved DNA substrate was verified by agarose gel electrophoresis in a 1.3% agarose gel at 90 V.

The primers were purchased from Stab Vida, with the following sequences:

Forward primer: 5’ CAGGTTCCGTCTTCCTCCAC 3’

Reverse primer: 5’ AAGAGGATGGAGAGGTGGCT 3’

GCAGCTTGTGGCCTGGGTCACCTCTACGGCTGGCCCAGATCCTTCCCTGCCGCCTCCTTC

AGGTTCCGTCTTCCTCCACTCCCTCTTCCCCTTGCTCTCTGCTGTGTTGCTGCCCAAGGA

TGCTCTTTCCGGAGCACTTCCTTCTCGGCGCTGCACCACGTGATGTCCTCTGAGCGGATC

CTCCCCGTGTCTGGGTCCTCTCCGGGCATCTCTCCTCCCTCACCCAACCCCATG/CCGTCT

TCACTCGCTGGGTTCCCTTTTCCTTCTCCTTCTGGGGCCTGTGCCATCTCTCGTTTCTTA

GGATGGCCTTCTCCGACGGATGTCTCCCTTGCGTCCCGCCTCCCCTTCTTGTAGGCCTGC

ATCATCACCGTTTTTCTGGACAACCCCAAAGTACCCCGTCTCCCTGGCTTTAGCCACCTC

TCCATCCTCTTGCTTTCTTTGCCTGGACACCCCGTTCTCCTGTGGATTCGGGTCACCTCT

Figure 4: Target region of CRISPR-Cas9 to be amplified with the primers in red and “/” as the cut site of Cas9.

3.10. CRISPR-Cas9 cleavage assay in HEK cells

HEK cells, were cultured in 24 well-plates for posterior transfection of the CRIPSR-Cas9 complex, using Lipofectamine 2000 (Invitrogene). The 100 µM solutions of crRNA and trancrRNA prepared in *In vitro* CRISPR-Cas9 cleavage assay, were used to form the gRNA duplex, by adding to a PCR tube, 8 µL of nuclease-free water, 1 µL of crRNA and 1µL of trancrRNA and consequently incubated for 5 min. in dry bath, at 95 ºC. The duplex was diluted with RNase-free water to a final concentration of 1 µM. The stock solution of Cas9 was also diluted to reach 1 µM. It was mixed 3 µL of gRNA, 3 µL of Cas9 and 44 µL of simple medium (DMEM). It was prepared CRISPR-Cas9 complex with our guide, a positive control and a negative control. In another Eppendorf, 2 µL of lipofectamine 2000 were diluted in 48 µL of simple medium (DMEM). Both these mixes were incubated for 5 min. in room temperature and afterwards mixed together and incubated at the same temperature, for 20 min. To finalize, it was added to the mix, 100 µL of simple medium (DMEM) and the solution was added to the cells and incubated at 37 ºC for 7h. After 7h the medium was replaced by complete medium (DMEM medium, 10% FBS, 1% PENSTREP (GIBCO™)) and 48h were needed for CRISPR-Cas9 complex to act. Cells were washed with PBS 1X, detached with 0.05% trypsin, and incubated at 37 ºC for 3 min., cells before being released from the surface. 200 µL of medium were used to resuspend the cells before centrifugation at 1200 rpm for 5 min. Supernatant was removed and pellet of cells was conserved at -80 ºC for future use with GeneArt kit. Following GeneArt step, it was mixed 50 µL of cell lysis buffer and 2 µL of protein degrader and 50 µL of such mix was used to resuspend cell's pellet for further transfer to PCR tubes. In the thermocycler, the following program was used:

Table 8: Cell lysis and protein denaturation program.

68ºC	15 min.
95ºC	10 min.
4ºC	Hold

The lysate was vortexed for further mix in a PCR tube, 2 µL of cell lysis, 1 µL of each primer (10 µM), 21 µL of Nuclease-free water and in the end, 25 µL of AmpliTaq Gold ® 360 MasterMix. The following amplification program was used:

Table 9: PCR program for DNA substrate amplification.

Enzyme activation	15 ºC	10 min.	1X
Denaturation	95 ºC	30 sec.	40X
Anneal	68 ºC	30 sec.	
Extend	72 ºC	30 sec.	
Final Extend	72 ºC	7 min.	1X
Hold	4 ºC	Hold	1X

An agarose gel of 1.2 % was made to verify the correct amplification. 2µL of PCR product was mixed with 1 µL of 10X Detection Reaction Buffer and Nuclease-free water was added to reach 9 µL. The following re-annealing program was used:

Table 10: Re-annealing program.

95 ºC	5 min.
95-85 ºC	-2 ºC/sec.
85-25 ºC	-0.1 ºC/sec.
4 ºC	Hold

1 µL of Detection Enzyme was added and the solution was incubated at 37 ºC for 1h. An agarose gel of 1.2 % was made to verify the correct if there was cleavage in the appropriated locations, by the band's sizes.

4. Results

4.1. Optimization of the microporation conditions in all-in-one Cas9 plasmid

Previous results from our group had demonstrated that MSC cells transfected with pX459 (pSpCas9(BB)-2A-Puro, Addgene plasmid #62988), where a custom-designed guide RNA sequence targeting the AAVS1 locus has been cloned, were highly susceptible to selection to puromycin. Therefore, an attempt to optimize the parameters for microporation was performed with pX458 (Addgene at # 48138), using the EGFP as a reporter for the success of the transfection.

For that, 100 000 cells were used for each condition. Different voltages were used ranging from 850 to 1600 V, with pulse widths ranging from 10 to 30 ms in 1 to 3 pulses (Table 11).

Table 11: All conditions used in optimization of microporation.

Condition Name	Voltage	Pulse Width (ms)	Pulse Number
A1 (Control)	No microporation		
A2	1400	20	1
A3	1500	20	1
A4/A5	1650	20	1
A6	1100	30	1
B1	1200	30	1
B2	1300	30	1
B3	1400	30	1
B4	1000	40	1
B5	1100	40	1
B6	1200	40	1
C1	1100	20	2
C2	1200	20	2
C3	1300	20	2
C4	1400	20	2
C5	850	30	2
C6	950	30	2
D1	1050	30	2
D2	1150	30	2
D3	1300	10	3
D4	1400	10	3
D5	1500	10	3
D6	1600	10	3

After microporation, cells were left to recover for 48h. The condition with highest number of fluorescent cells was that of cells transfected with a voltage of 1400 V, a pulse width of 30 ms in 1 pulse. In a similar condition with 1300 V, fluorescence was the second highest (Figure 5). With the resultant cells, flow cytometry was performed for relative quantification of fluorescent and cell viability. The previously top condition was once again the one with highest fluorescence (31%), but the cell viability was really reduced, surviving just 5000 viable cells. Condition 1300 V, 30 ms, 1 pulse showed second best fluorescence levels and greater number of cells viability (16,6 % and 20 800 viable cells). Unfortunately, these statistics aren't

trustworthy since flow cytometry was run with a number of events inferior to the minimum advised (100 000 cells).

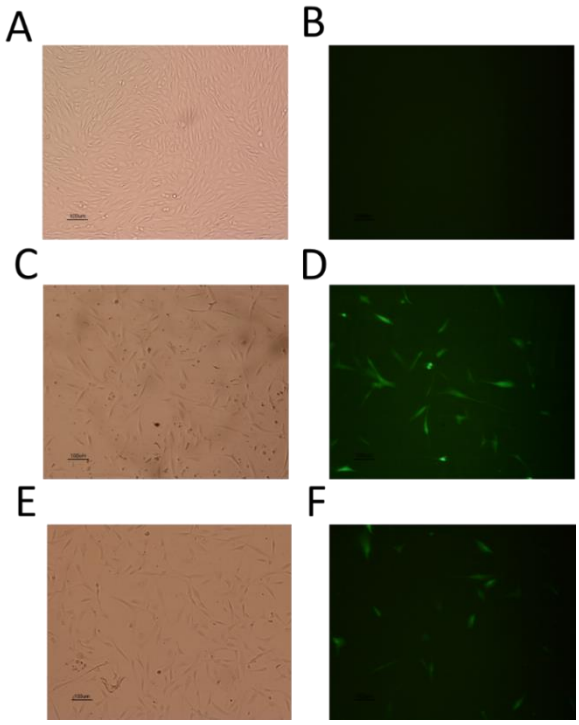

Figure 5: Fluorescence microscopy of MSCs microporated with all-in-one plasmid. **A:** Control (not microporated) in white light. **B:** Control in fluorescence microscopy **C:** Conditions 1400 V for 30 ms in 1 pulse in white light. **D:** Conditions 1400 V for 30 ms in 1 pulse in fluorescence microscopy. **E:** Conditions 1300 V for 30 ms in 1 pulse in white light. **F:** Conditions 1300 V for 30 ms in 1 pulse in fluorescence microscopy.

After establishing these conditions, MSC cells were microporated with pX459 where the custom-designed guide RNA had been cloned, using the conditions 1400 V for 30 ms in 1 pulse and 1300 V for 30 ms in 1 pulse. Several attempts were made to improve cell survival upon selection with puromycin, however, all failed. Both microporation conditions were tested and cells were cultured with the following puromycin concentrations: 0.1, 0.25 and 0.5 µg/mL. Unfortunately, cells died or the time of culture needed would lead to a not observable cut, having the different conditions, identical results.

4.2. Optimization of 6-His-MBP-Cas9-mCherry production in *E.coli* BL21(DE3)

Firstly, to edit the genome of the MSCs, the CRISPR-Cas9 tool must be produced in quantity, in order to later transformation of the complex in the cells. *E.coli* BL21(DE3) was used for over-expression of Cas9 protein, by transformation of this strain through electroporation with pMJ923 plasmid (Addgene plasmid # 78313, a kind gift from Martin Jinek, Annex 1), a vector that encodes for Cas9 protein in which overexpression is induced by with IPTG. In this plasmid, Cas9 is fused with mCherry, MBP (for higher solubility) and 6 His (tag for purification). This plasmid was extracted from *E.coli* DH5α, quantified with Nanodrop and transformed into competent *E.coli* BL21(DE3) by electroporation. Cultures in selective medium (with ampicillin) were made with the resultant transformed bacteria, and one colony was further cultured in petri diches for cell stock.

To test the expression of Cas9 at different temperatures, cell cultures were induced by IPTG and incubated at different temperatures: 37, 30, 25, and 20 º C. Samples were acquired at 0, 2 and 4 hours after induction, depending on the tested temperatures. The protein samples were separated in SDS gels (Figure 6) and visualized by Western blots (Figure 7), to see the over-expression of Cas9.

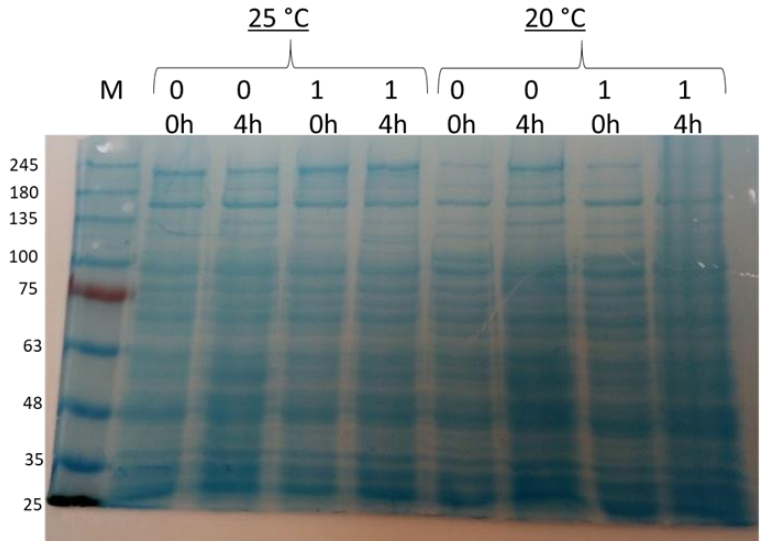

Figure 6: 8% SDS-PAGE gel of samples at time 0h and 4h of culture with (1) or without (0-control) IPTG (1mM) at 25 °C and 20 °C.

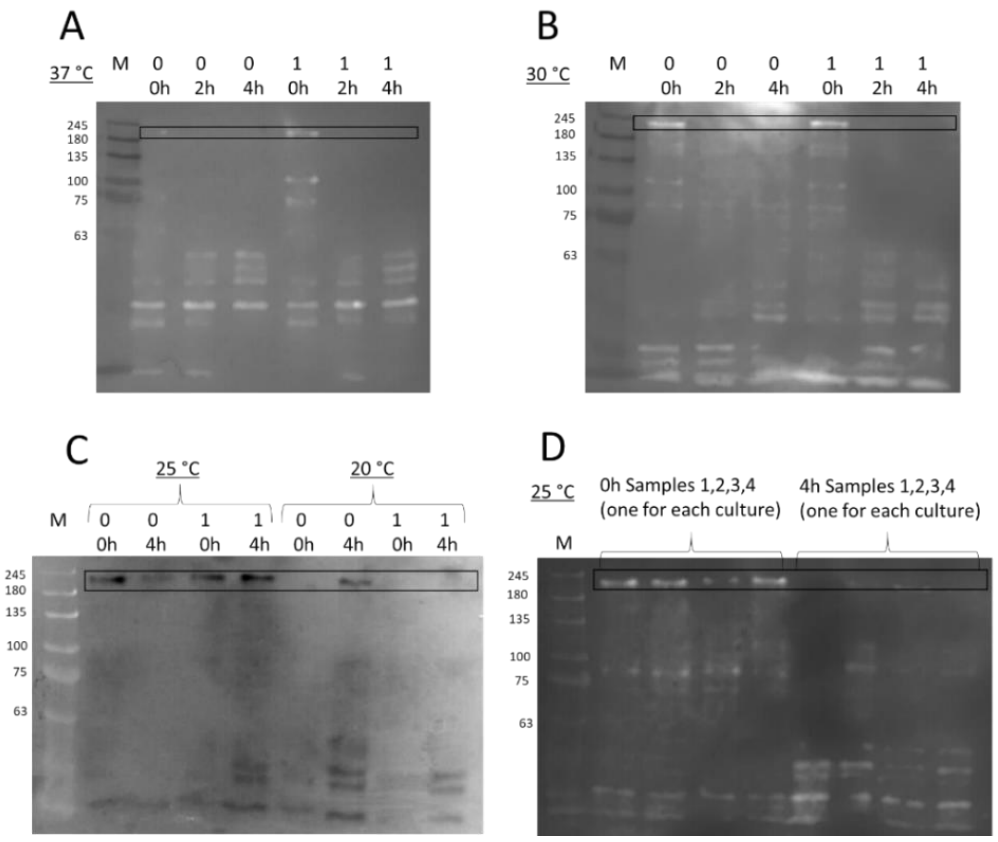

Figure 7: Western blots made with antibodies for 6-Histidine of Cas9 produced at 37, 30, 25 and 20 ºC. 0 represents no IPTG and 1 represents addition of IPTG (1mM). The molecular weight of mCherry-Cas9-6His-MBP is approximately 230 kDa (6His = 1kDa, SpCas9 = 158, MBP = 42 kDa, mCherry = 29 kDa) and the dark sections indicate the location of the Cas9 fusion protein. **A:** Western blot of samples of 0h 2h and 4h of culture with (1) or without (0-control) IPTG at 37 °C; **B:** Western blot of samples of 0h 2h and 4h of culture with (1) or without (0-control) IPTG at 30 °C; **C:** Western blot of samples of 0h and 4h of culture with (1) or without (0-control) IPTG at 25 °C and 20 °C; **D:** Western blot of samples of 0h and 4h of culture, all with (1) IPTG at 25 °C, the determine best conditions until then.

The results of samples taken after different hours of culture showed an apparent decrease of Cas9 production through time which was initially thought to be due to toxic effects of Cas9 overexpression in bacteria. Therefore, lower IPTG concentrations were tested (0, 0.2 and 0.5 mM) in culture for Cas9 production and 18 ºC and 25 ºC temperatures were also tested in longer periods after induction, namely of 0, 6h and overnight (O.N.) (Figure 8). The results showed over-expression of Cas9 in all conditions at 25 °C with the higher productivity present in the culture where 0.2 mM of IPTG were used (Figure 8B). At 18 °C, the higher production was also showed in concentration 0.2 mM.

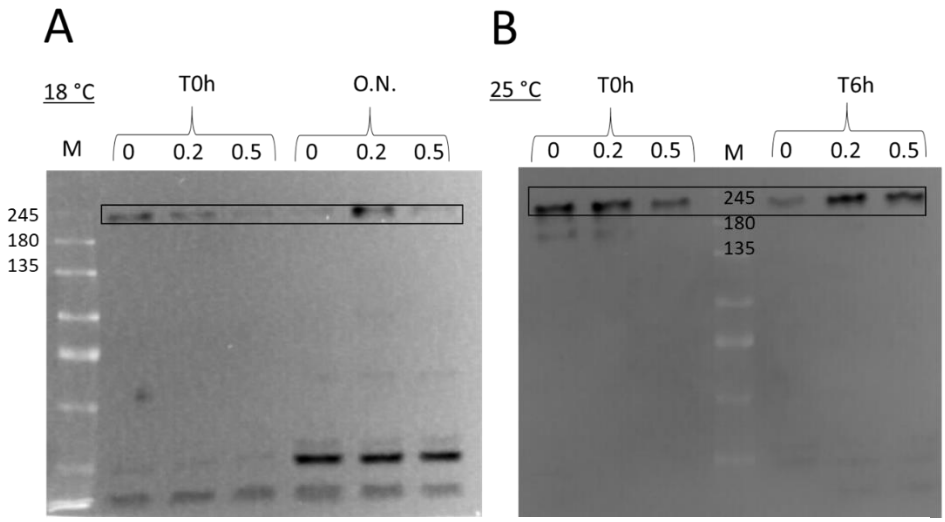

Figure 8: Western blots of Cas9 production with different concentrations of IPTG (no IPTG, 0.2mM and 0.5 mM). **A:** Tested at 18 °C at time 0h and after overnight growth. **B:** Tested at 25 °C at time 0h and after 6h of growth.

With all the previous experiments testing different temperatures and IPTG concentrations, we concluded with effect, that the best conditions for Cas9 production in this *E.coli* strain, is at 25 ºC, using 0.2 mM of IPTG. After reaching the conclusion that 25 °C was the best temperature, 8.250 L of culture were produced for further sonication and purification (Figure 9).

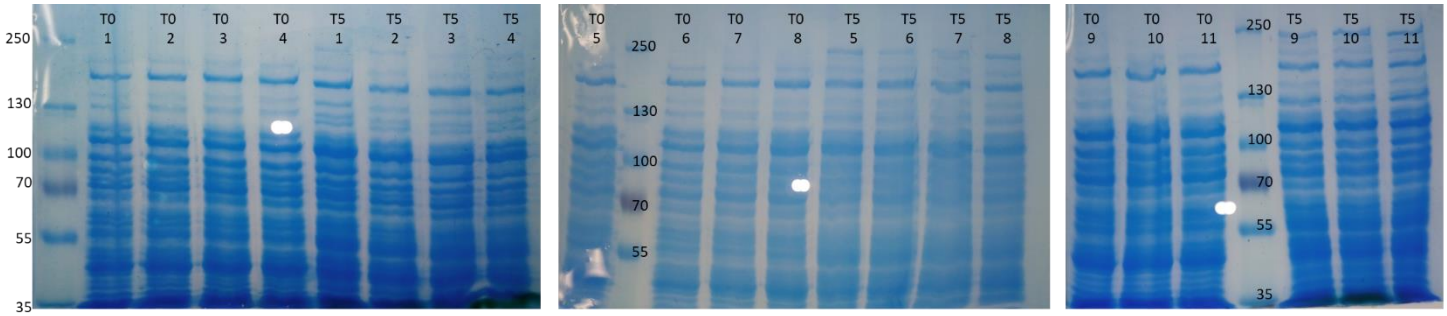

Figure 9: 8% SDS gels of samples of the eleven cell suspensions of 750 mL needed to reach 8.250 L for future purification. All suspensions were induced with 0.2 mM of IPTG and cultured at 25 ºC for 5h after induction. T0 represents 0h of induction. T5 represents 5h after induction.1-11 represents each culture. New band of 230 KDa observed after 5h of induction in all cultures, representing the Cas9 fusion protein.

4.3. Production of TEV

In the process of Cas9 purification, a step needed to maintain the functionality of the protein is the cleavage of 6 His-MBP out of the Cas9 fusion protein. For such purpose, the Cas9 fusion protein has a TEV recognition sequence in which TEV protease will cleave. TEV protease had to be therefore, produced and purified for use in Cas9 purification.

E. coli BL21(DE3) transformed with pRK793 plasmid (Addgene plasmid # 8827) was used for over-expression of TEV with IPTG 1mM induction. The fusion protein is expressed as MBP-His6-TEV(S219V)-Arg5. The MBP is present in this fusion protein in order to increase solubility, maintain active state of the protease and inhibit formation of inclusion bodies. Incubation of 2L of cell suspension were performed at 30 ºC, at 250 rpm, for 5h and 12% SDS gel was made in the end with samples taken at 0 and 5 h after induction (Figure 10A). The resultant gel, after 5h of induction with IPTG (1mM), shows the appearance of two new bands, one of 42 KDa that represents MBP self-cleaved *in vivo* by the presence of TEV sequence in the fusion protein (Figure 10B), and a band close to 29 KDa representing the His6-TEV(S219V)-Arg5 protease.

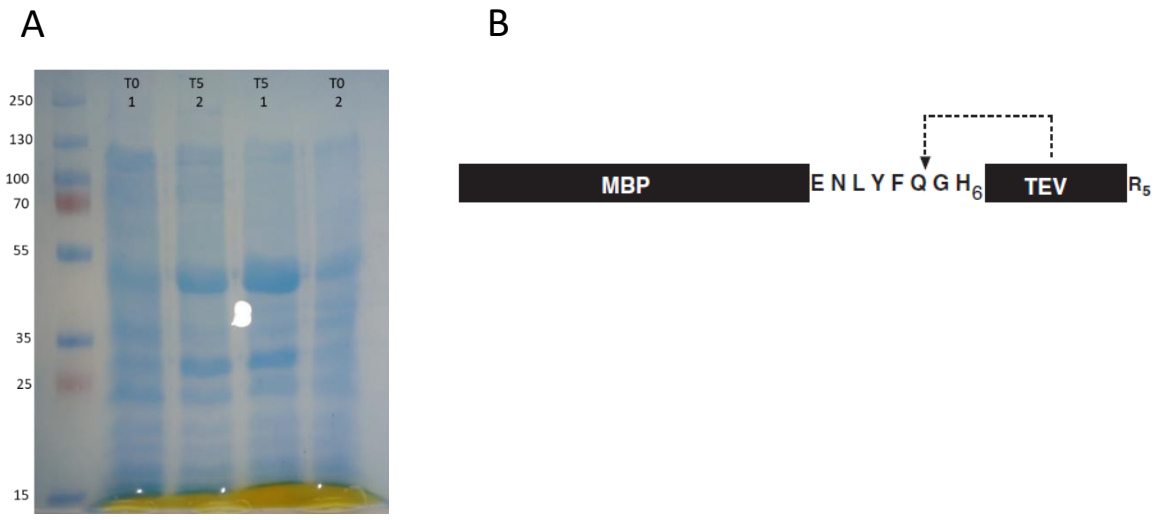

Figure 10: TEV expression and self-cleavage in *E. coli.* **A:** 12% SDS gel of TEV production in *E. coli* BL21(DE3). Protein overexpression of two cultures (1 and 2) was induced with IPTG (1mM). T0 represents 0h after induction and T5 represents 5h after induction. **B:** Structure of TEV fusion protein and self-cleavage for MBP release to maintain functionality [112]

4.4. Purification of TEV

The cells from 2L of culture were lysed by sonication before IMAC (Immobilized Metal Affinity Chromatography) was performed in a HisTrapTM FF 5 mL, (GE Healthcare).

As seen in the chromatogram of IMAC purification (Figure 11A), one big spike in the absorbance at 280nm is observed in the elution step, which should represent TEV protease. Samples of the enriched fractions were taken and a 12% SDS gel was made to observe if the spike corresponded effectively to the TEV protease (Figure 11B).

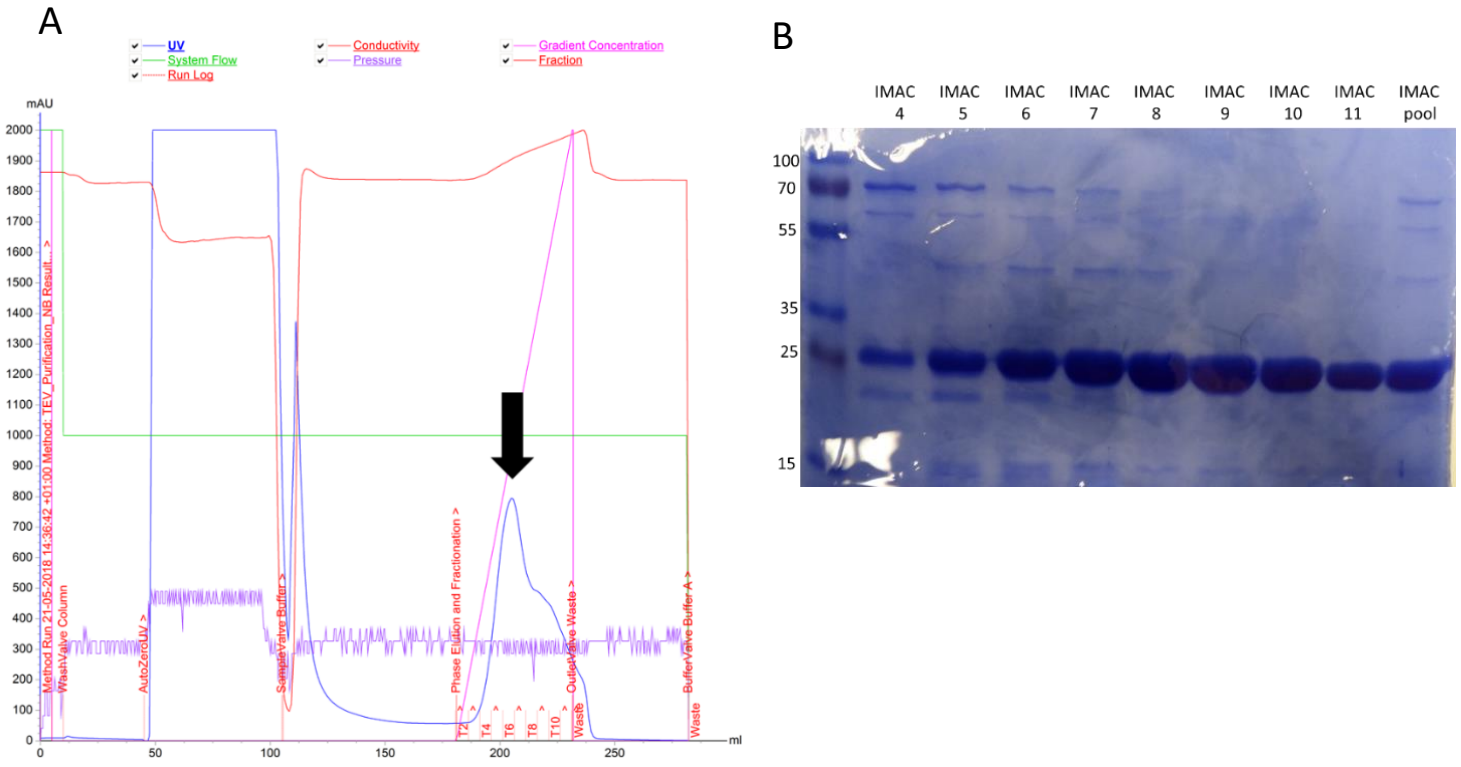

Figure 11: TEV purification with IMAC. **A:** Chromatogram resultant of IMAC with nickel for TEV purification. **B:** 12% SDS gel of TEV rich fractions of IMAC purification. 4-11 represent the number of the elution fractions of the chromatogram. Pool refers to the sample of the mix of all rich fractions.

TEV protease was further purified in a gel filtration. The resultant chromatogram showed a big spike, assumed to be TEV protein (Figure 12A). 12% SDS-PAGE gels were run with the samples of the spike to verify the purity of the protein (Figure 12B). Strong bands appeared close to 29 KDa, the size of TEV in IMAC and Gel filtration gel, showing that effectively TEV protease was in monomers. The enriched fractions were once again concentrated, reaching 9µM of TEV protease in the end (3.78 mg/mL).

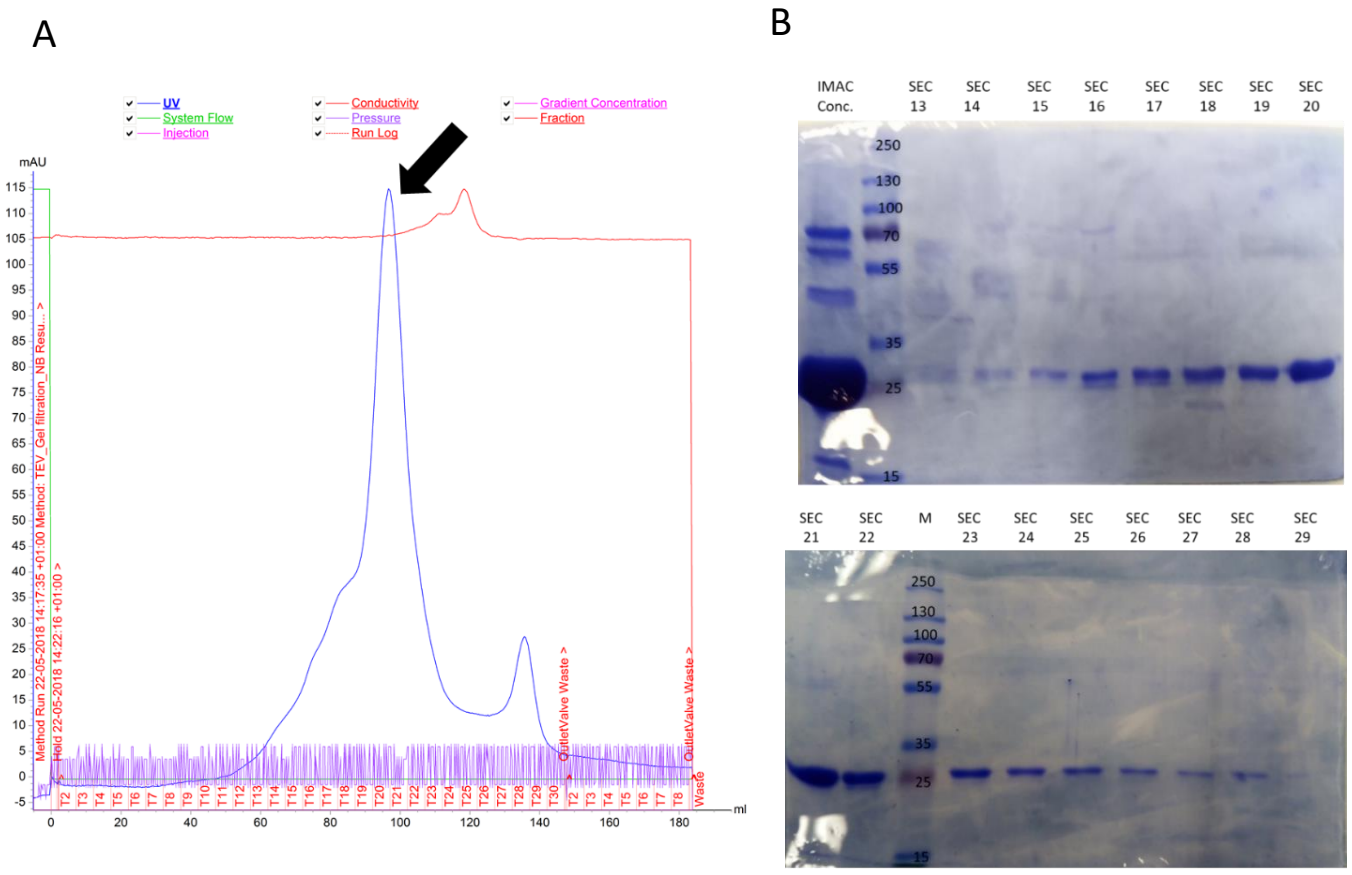

Figure 12: TEV purification with Gel filtration. **A:** Chromatogram resultant of Gel filtration for TEV purification. **B:** 12% SDS gels of TEV rich fractions of Gel filtration. 13-29 represent the number of the elution fractions of the chromatogram. IMAC conc. refers to the sample of concentrated IMAC rich fractions right before Gel filtration.

4.5. Purification of Cas9-mCherry

Initially the process of purification of Cas9 is very similar to the TEV purification, in which the resultant cells of the 8.250 L of culture were lysed by sonication and IMAC (Immobilized Metal Affinity Chromatography) was performed in a HisTrapTM FF 5 mL, (GE Healthcare). The chromatogram of IMAC shows a sharp spike assumed to be the Cas9 fusion protein (Figure 13A). Confirmation of the identity of the spike was made in an 8% SDS-PAGE gel of the enriched fractions of the spike (Figure 13C). Furthermore, after purification the fractions associated to this spike presented a strong pink color in the glass tubes suggesting the presence of mCherry released light by the fusion protein.

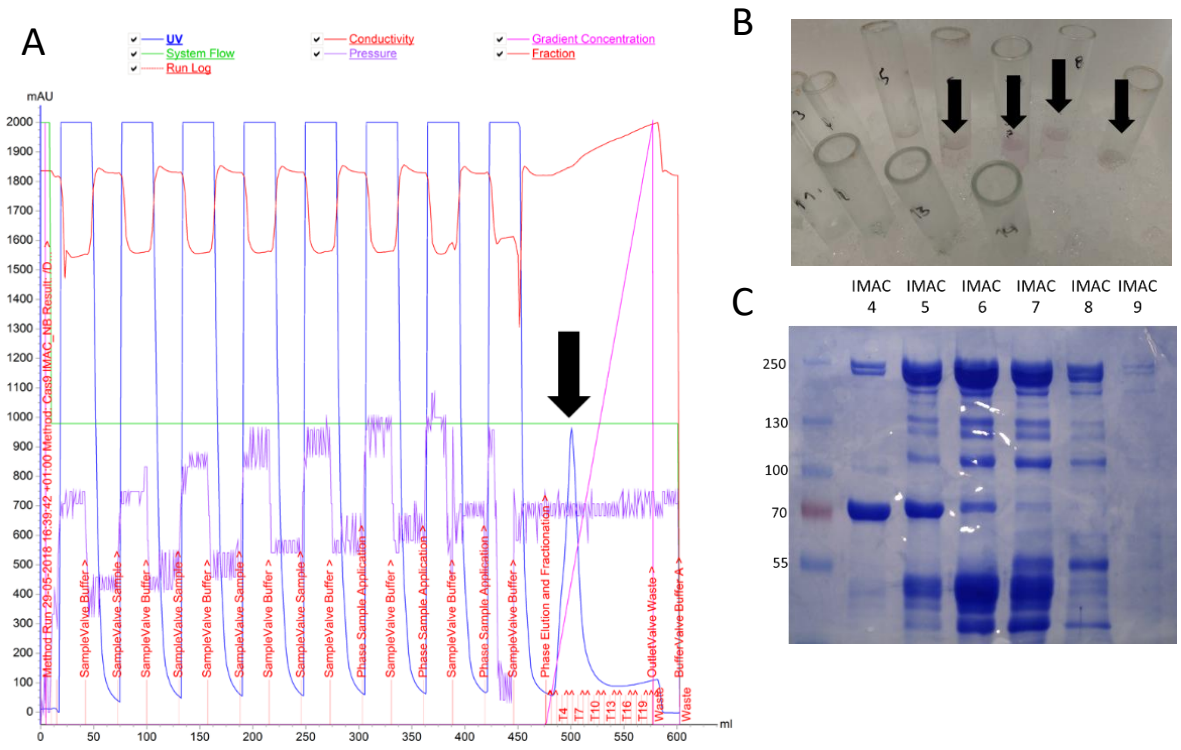

Figure 13: Cas9 purification with IMAC. **A:** Chromatogram resultant of IMAC with nickel for Cas9 purification. **B:** Glass tubes with Cas9 rich fraction emitting pink light due to mCherry. **C:** 8% SDS gel of Cas9 rich fractions 4-9.

The gel showed strong bands of 230 kDa in the samples corresponding to the spike, representing 6-His-MBP-Cas9-mCherry. These rich fractions (4-10) were concentrated with 10,000 MWCO Amicon (Milipore) for further Dialysis to remove imidazole from the purification and combined 6 His-MBP cleavage with TEV in a Dialysis cassette (ThermoFisher SCIENTIFIC). The concentrated sample was divided for two dialysis cassettes for a better ratio between Cas9 sample and TEV. In one, 3 mL of Cas9 were cleaved with 900 µL of TEV produced, while in the other, 3.7 mL of Cas9 were cleaved with 600 µL of TEV. The two tested quantities of TEV showed in both, almost 100% efficiency in cleavage after 40h to 64h of incubation at 4 ºC, while dialysis was occurring for imidazole removal. This phenomenon was visualized by the shift of Cas9 band of 230 to 187 kDa in the 8% SDS gels of Figure 14. The two resultant solutions of cleaved Cas9 were concentrated together in order to reach the volume indicated for IEX (Ion Exchange) Chromatography.

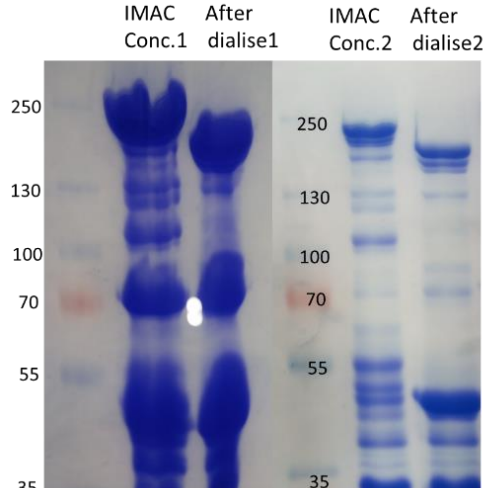

Figure 14: 8% SDS gel of Cas9 Dialysis and 6 His-MBP cleavage. 1 represents the cassette with 3 mL of Cas9 and 900 µL of TEV. 2 represents the cassette with 3.7 mL of Cas9 and 600 µL of TEV.

The resultant chromatogram of IEX (Figure 16), shows two spikes at approximately 20% and 30% of Buffer B while a final manual run with 100% elution buffer shows another spike. 8% SDS gels of the enriched fractions of each spike allowed the verification of protein purity. The manual run was executed since pink color was observable even after the end of the program, showing thus, that some Cas9 was still trapped inside the column (Figure 15).

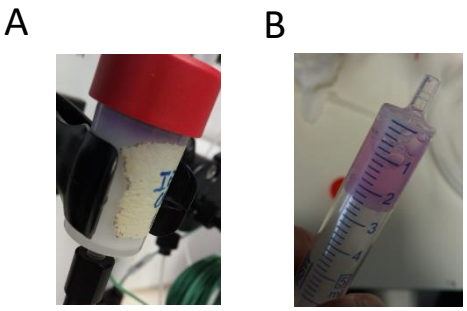

Figure 15: Observable pink gradient of Cas9. **A:** IEX column with observable pink gradient in top after sample loading and washout. **B:** Concentrated IEX rich fractions with strong pink color, an indicative of high Cas9 concentration.

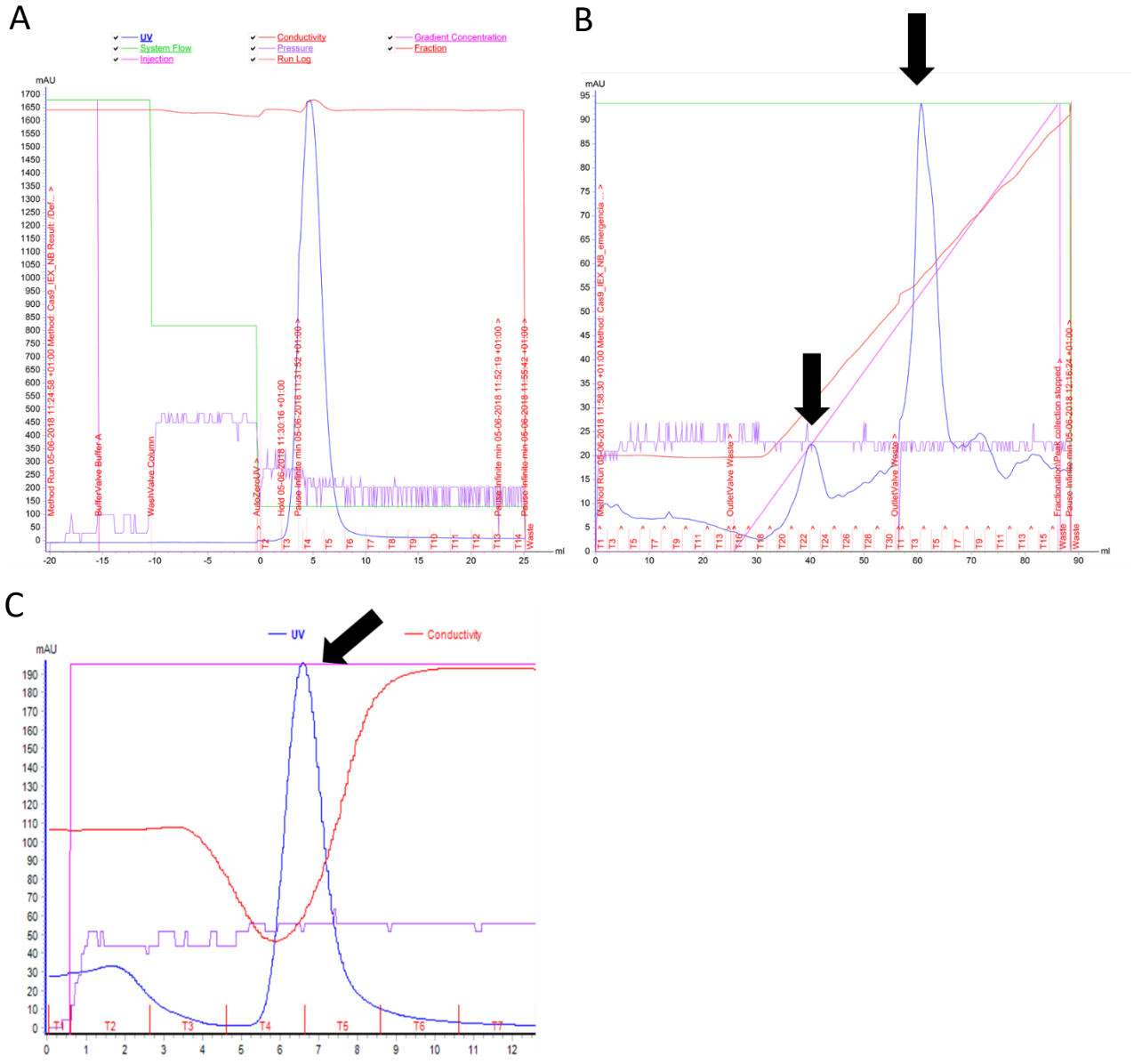

Figure 16: Chromatograms of IEX of Cas9. **A:** Chromatogram of IEX Sample loading and Washout. **B:** Chromatogram of IEX Elution. **C:** Chromatogram of IEX manual run with 100% Elution buffer.

The 8% SDS gels demonstrated no Cas9 protein in the first spike, while in the second spike showed high Cas9 concentrations with high purity in most fractions in the 187 kDa bands (Figure A-D). The samples 4 and 5 of the manual run showed also enrichment in Cas9 with less but still good level of purity. The samples 28 to 38 and EM 5 and 6 were concentrated together until 500 µL for further purification with SEC (Size Exclusion Chromatography) too remove mostly the small proteins still present in the sample.

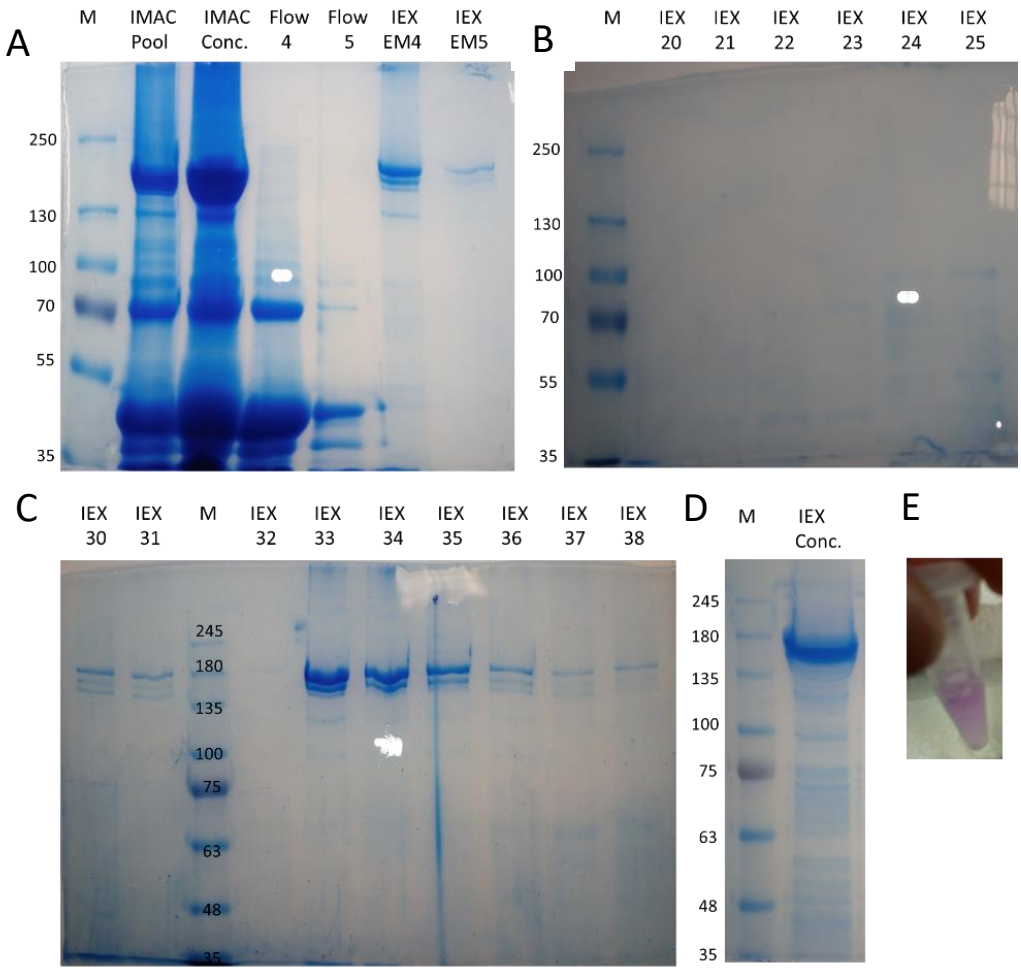

Figure 17: SDS gels of Cas9 purification with IEX. **A:** 8% SDS comparing pool and concentrated of rich fractions of IMAC, Washout 4 and 5 (to verify if there was lost of Cas9 in such step) and sample 4 and 5 of manual run (spike of manual run). **B:** 8% SDS gel of fractions 20-25 (first spike) of IEX. **C:** 8% SDS gel of fractions 30-38 (second spike) of IEX. **D:** 8% SDS gel of IEX concentrated. **E:** Eppendorf of concentrated IEX rich fractions with strong pink color due to mCherry of Cas9, thus showing high concentration.

Quantification of Cas9 in the concentrated sample of IEX rich fractions, was made with spectrophotometry using a wavelength of 280 nm and an extinction coefficient of 120,450 M^{-1} cm^{-1} [42] to estimate protein concentration. The quantification was done with dilution 1/10 in order to maintain inside of the range method and for minimal waste of Cas9. The graph showed two spikes as predicted, one at 280 nm, describing Cas9 and another one at 587 nm, the excitation spike of mCherry fluorescence (Figure 18). After calculations with the absorbance at 280 nm, the concentration determined for the sample of concentrated Cas9 without dilution, was 15 µM, using the Lambert-Beer Law.

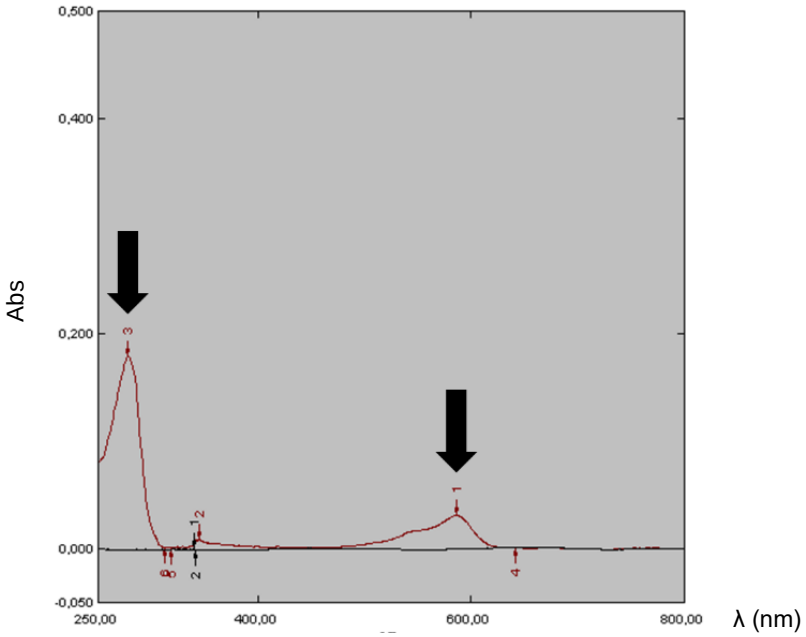

Figure 18: Graphic of absorbance through wavelength of concentrated IEX rich fractions with 1/10 dilution. 280 nm spike of Cas9 and protein contaminants and 587 nm spike of excitation wavelength of mCherry.

SEC was performed, resulting in a chromatogram with two great spikes that correlated with pink elution from column (Figure 19B). After 8% SDS-PAGE gel, the two spikes were revealed as being effectively Cas9 plus some bands of close size with chances of being Cas9 degraded or protein contaminants of similar sizes and properties, that we were unable to separate (Figure 20A-B). Rich fractions (13-21) were then concentrated and a new 8% SDS gel and Cas9 quantification was made, reaching 6 µM of Cas9-mCherry (Figure 20C).

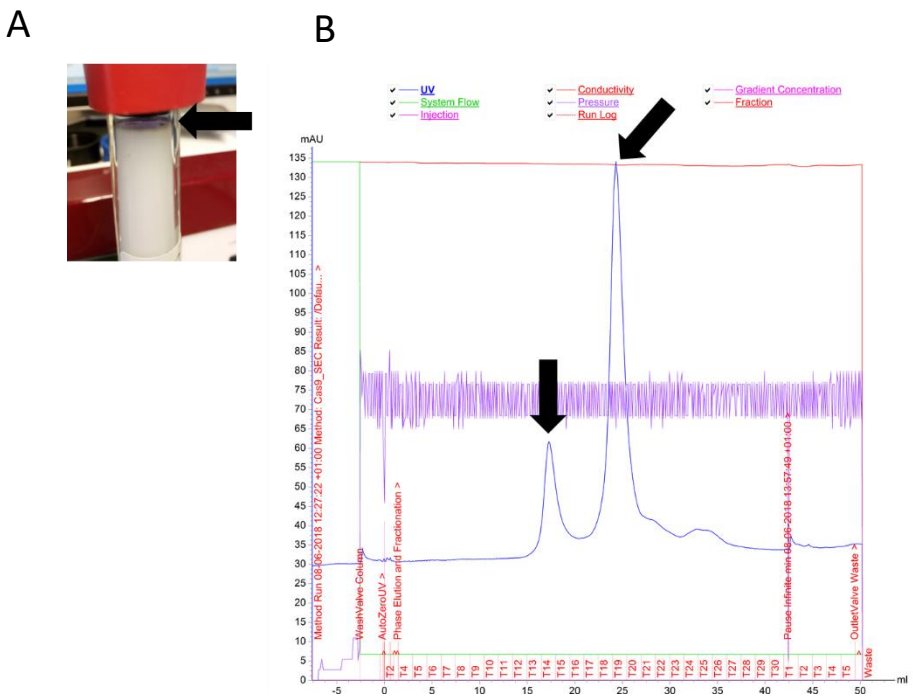

Figure 19: Cas9 purification with SEC. **A:** SEC column with pink from mCherry-Cas9. **B:** Chromatogram of SEC Elution.

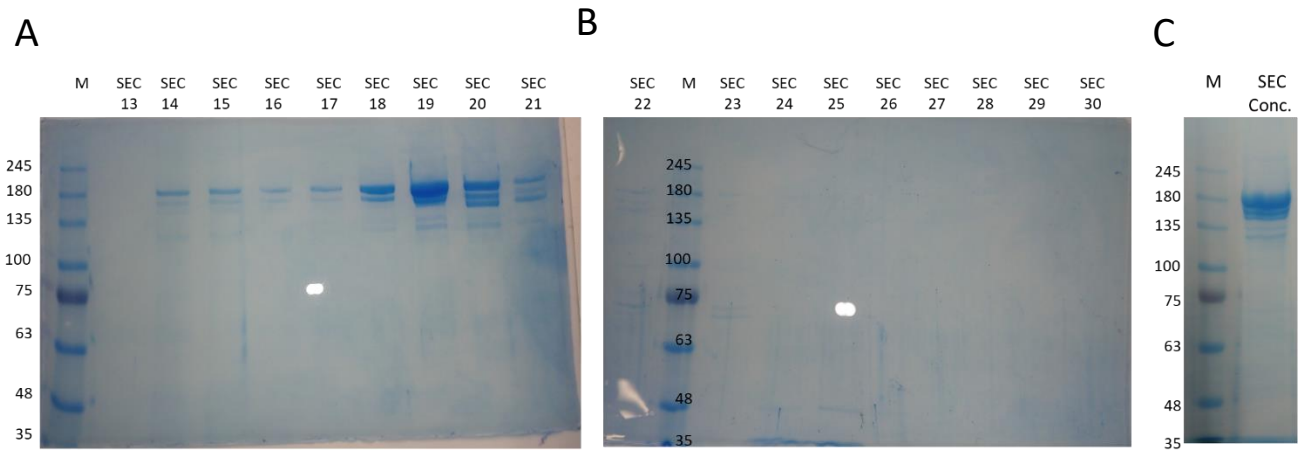

Figure 20: SDS gels of SEC purification. **A and B:** 8% SDS gels of SEC fractions. **C:** 8% SDS gel of concentrated rich SEC fractions 13-21.

4.6. *In vitro* cleavage assay of CRISPR-Cas9 complex

After production and purification of Cas9 protein, a cleavage test *in vitro* is needed to confirm the functionality of the produced protein. HEK, HeLa and AT-MSCs (Adipose tissue-derived MSCs) were cultured for DNA extraction and consequently, amplification by PCR of the target region for CRISPR-Cas9 edition, the first intron of the *PPP1R12C* gene (phosphatase 1 regulatory subunit 12C), located in a recognized genomic safe harbor of chromosome 19.

The PCR was performed, and a 1.3% agarose gel was run with the PCR product. The PCR product showed only one band in all PCR products of the three types of human cells as predicted, with a size of 372 pb, the size of the targeted region meant to be amplificated (Figure 21A).

After the amplification of the DNA target region, an *in vitro* cleavage assay was performed with purified Cas9 protein. The gRNA duplex was assembled with specific crRNA and trancrRNA from IDT (Integrated DNA Technologies) before being complexed with the Cas9-mCherry to produce the RNP complex. The results showed efficient cleavage of the DNA substrate, close to 50%. However, a band of 400 bp representing the DNA substrate uncleaved, and two bands close to 175 and 197 pb, the size of the fragments produced by cut in the right place are seen (Figure 21B). It is observable that the uncleaved band after cleavage is higher in the gel. This is possibly due to a not 100% release of the RNP complex from the DNA substrate, thus increasing the molecular weight of the fragments.

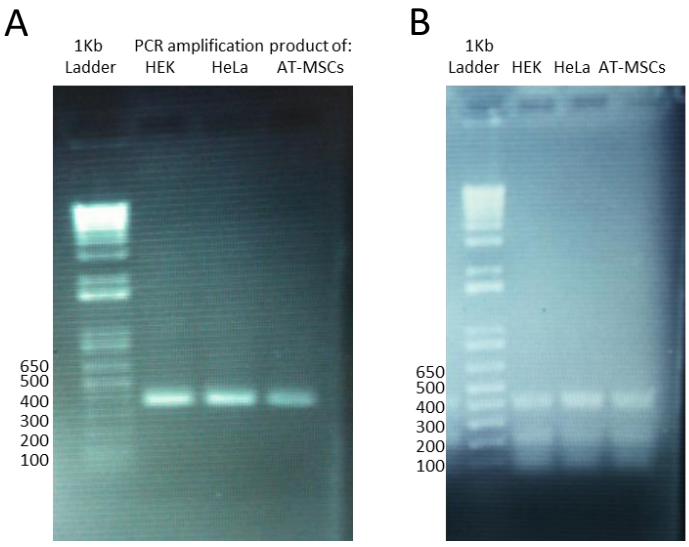

Figure 21: 1.3% Agarose gels of cleavage assays *in vitro* **A:** PCR product of target region of HEK, HeLa and AT-MSCs **B:** CRISPR-Cas9 cleavage assay in the PCR product of target region of HEK, HeLa and AT-MSCs.

4.7. Cleavage assay of CRISPR-Cas9 complex in HEK cells

Upon observing successful DNA cuts *in vitro* we continued the study in cultured cells *in vitro*, to observe if the same efficiency would be observed within the cells. HEK cells were first tested, since they are of human origin, and are easily transfectable. The cells were transfected with the *in vitro* assembled RNP complex, using Lipofectamine 2000. Three different complexes were construct, one with the guide2 for targeting the safe harbor and positive and negative control kits from IDT (Alt-R™ CRISPR-Cas9 Control kit Human). Cells were transfected and after 48h, were pelleted for lysis with GeneArt kit lysis buffer (Invitrogen). Like in the *in vitro* test, the target region was amplified with PCR and separated on an agarose gel (Figure 22A). A band close to 372 bp for guide 2, and a band close to 1083 bp in both controls were visualized as predicted, showing effective amplification of the target regions. Within the cells, after cleavage, the DNA is repaired most of the times by NHEJ, therefore InDel mutations are added to the DNA sequence. By denaturating and re-annealing, both wt and mutated sequences are put together in the final DNA product, which after incubating with the cleavage detection enzyme (not disclosed in the kit), results in a cleaved PCR product, producing two bands of the predicted sizes (Figure 22B). It is possible that due to the similarity in sizes of the fragments produced by guide2, only one band is observable due to low resolution of the gel. The band of PCR amplification was also well observed in the three samples. The positive control appears also with two new bands (827 and 256 pb) with the predicted size, showing effective cleavage. The negative control maintained only the PCR amplification band as predicted.

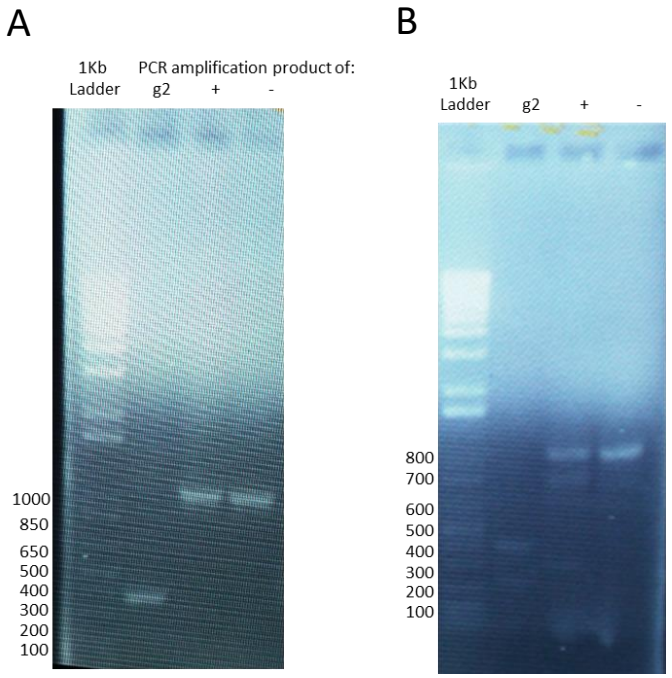

Figure 22: 1.2% Agarose gels of cleavage assays in HEK. **A:** PCR product of target regions of HEK. **B:** CRISPR-Cas9 cleavage assay in the PCR product of target region of HEK.

5. Discussion

In the development of this novel cell-based therapy against cancer, MSCs will be engineered with a transfectable RNP CRISPR-Cas9 complex assembled *in vitro* and a donor template, to express and secrete azurin protein. The inherent tropism to cancer cells of the MSCs together with the anti-cancer properties of azurin, have the potential to generate a new therapy against cancer.

The best conditions for the microporation of MSC were observed to be at a voltage of 1400 V, with a pulse width of 30 ms in 1 pulse and a similar condition with the variant of 1300 V instead of 1400 V. The first showed highest fluorescence, thus higher efficiency in transfection, however, the viability was extremely poor. The second condition even though it had less fluorescence, it had greater viability.

Even though, the microporation conditions were optimized to MSCs with the all-in-one plasmid, selection with puromycin showed negative results, thus clarifying that the problem was not in the aggressiveness of microporation, but in the puromycin. It also shows one more time that RNP transfection is a better solution, since it thus not need selection with antibiotics.

The second step of this study was the effective production of Cas9 in *E. coli* BL21 (DE3). Due to the exogenous nature of this protein, different proteins are expressed in response. When comparing SDS gels of Cas9 and TEV proteins, it is clear that there are different protein expressions even though the strain is the same and culture conditions are identical. After IMAC it is possible to observe that the purification of TEV is highly efficient when compared to IMAC of Cas9. This suggests that the proteins expressed by response of Cas9 are richer in histidine, making purification harder.

This is also consequence of the nature of proteome of *E. coli* BL21 (DE3). Recombinant His-tagged proteins expressed in this strain are commonly coeluted with native *E. col*i proteins in IMAC and this effect is increased specially when the expression of the recombinant protein is low, like the Cas9 protein. The native *E. col*i proteins have clustered histidine residues with metal binding sites. Such problem could be fix with engineered *E. coli* BL21(DE3) where the most dominant contaminants have alternative tags or mutations for affinity loss to nickel. [114] Alternatively, other strains can also be used like Rosetta strains since in some cases this strain is better suited for the expression of proteins of eukaryote origin.

In previous purifications, after dialysis and 6 His-MBP cleavage, IMAC was tried to run manually to separate cleaved from uncleaved Cas9 protein. Unfortunately, both forms had high affinity to the nickel, revealing that Cas9-mCherry is rich in histidine or other resides with affinity for nickel. A possible reason is that Cas9 HNH nuclease domain is most likely to employ a one-metal-ion mechanism for target-strand DNA cleavage, that is a conserved general base histidine. RuvC likely uses a two-metal-ion catalytic mechanism for cleavage of the nontarget DNA strand, based in conserved aspartate residue. [115]

Due to the toxicity of Cas9, it was also used an induction system with IPTG in order to limit exposure of cells and decrease suppressor mutations that inactivate Cas9. [116]

The ideal conditions for Cas9 protein in this system were culture at 25 ºC with 0.2 mM of IPTG. IPTG at high concentrations showed inhibition of Cas9 expression. This could be consequence of the reduction in growth rate and saturation due to higher IPTG concentrations. Also, the reduction in growth rate is higher in early exponential phase when compared to late exponential phase. [117]

Along purification, mCherry have emitted pink light even without laser excitation, and without even being exposed to almost no light. This is due to the fact that mCherry is from the group of red fluorescent proteins, also called permanently fluorescent proteins. [119] This transition begins when exposed to light in purification. Strangely, the color only appears later when storage in almost no light environment at 4 ºC, showing a possible slow activation maybe due to low temperatures. It is possible that imidazole of the elution buffer also influences since it is a key constituent of the fluorophore system of red fluorescent proteins such as mCherry, that is responsible for their pH sensitivity. [120] However, it has been already showed that mCherry is not very sensitive to pH variations, in terms of emitted fluorescence. [120]

After finishing purification, only contaminants with same afiinity, ionic perfil, and size have been maintain, sugesting that the possible contaminants may be Cas9 degraded.

The cleavage assay *in vitro* of the PCR product of HEK, HeLa and AT-MSCs, using the constructed RNP CRISPR-Cas9 showed maintenance of functionality even after defrost and refrost of the complex and the efficiency in DNA cleavage in the target site was close to 50% in all cases despite the DNA origin. By the size of the bands generated in agarose gel, it appears that the cuts were performed in the right location. The 50% percentage efficiency is assumed due to the same intensity of the bands of uncut DNA and cut DNA.

The cleavage assay performed in cultured HEK cells reveals a weaker efficiency compared to *in vitro* as expected, since the complex needs to enter the cells and reach the target DNA Still promising results were showed in the agarose gel of the cleavage assay using guide2. A weak band close to 200 bp was seen in this gel. Due to low resolution of the gel, the two supposed band most likely became undistinguishable owing to their close size (175 and 197 bp). Comparing the intensity of the PCR amplification band, with the cleaved, it is possible to assume an efficiency of cleavage close to 40%. Also, the possibility of CRISPR-Cas9 being still attached, could alter and increase the molecular weight of the bands. The positive control emerged with two smaller bands, besides the uncleaved, having the right sizes of 1083 bp (uncleaved), 827 bp and 256 bp. The negative control maintained the PCR amplification band only, as predicted.

Cleavage assay of MSCs was also performed using the same method used in HEK, with 8h of incubation with RNP guide2, using 4 µL of Lipofectamine 2000 instead of 2µL used in HEK, and with incubation overnight with 2 µL of Lipofectamine 2000 (Figure A4). Unfortunately, results were not adequate due to low efficiency of transfection in MSCs, using Lipofectamine 2000. Due to malfunction of the microporator, Lipofectamine 2000 strategy had to be used to test cleavage efficiency in HEK and MSCs. In case of MSCs, it is known that the best method for transfection is microporation as documented [121].

6. Conclusion and future prospects

This study established conditions for an in-house production of Cas9 protein in *E.coli* BL21(DE3) that proved to be functional when complexed with the gRNA. With a positive control and a gRNA under test, efficiencies close to 50% were observed *in vitro* and a 40% efficiency when tested in HEK cells, thus being a great tool for genome edition using CRISPR-Cas9 system. In assays where many tests must be made, purchasing Cas9 could became a great expense and limit the number of conditions, guides or MSC donors to be tested, thus having the capability to produce it efficiently can reduce cost of research and availability. In future, tests will be performed to compare the efficiency of a given gRNA across different MSCs donors and tissues of origin. Furthermore, by adding a repair template construct for the incorporation of azurin within the genome of MSC, measures of azurin expression will be done and co-cultured with tumor cells, in order to see the effect in cancer proliferation.

7. References

1. Louwen, Rogier et al. “The Role of CRISPR-Cas Systems in Virulence of Pathogenic Bacteria.” Microbiology and Molecular Biology Reviews: MMBR, 2014, 78(1): 74–88.

2. Wei, Xin et al. “Mesenchymal Stem Cells: A New Trend for Cell Therapy.” Acta Pharmacologica Sinica 2013, 34(6): 747–754.

3. Heino TJ, Hentunen TA., “Differentiation of osteoblasts and osteocytes from mesenchymal stem cells.” Curr Stem Cell Res Ther. 2008;3(2):131-45.

4. Dai, Linghui et al. “Different Tenogenic Differentiation Capacities of Different Mesenchymal Stem Cells in the Presence of BMP-12.” Journal of Translational Medicine, 2015,13, 200.

5. Pfützner, Andreas et al. “Mesenchymal Stem Cell Differentiation into Adipocytes Is Equally Induced by Insulin and Proinsulin In Vitro.” International Journal of Stem Cells, 2017, 10(2): 154–159.

6. Wu R, Liu G, Bharadwaj S, Zhang Y. “Isolation and myogenic differentiation of mesenchymal stem cells for urologic tissue engineering.” Methods Mol Biol., 2013; 1001:65-80.

7. Wislet-Gendebien S, Wautier F, Leprince P, Rogister B., “Astrocytic and neuronal fate of mesenchymal stem cells expressing nestin”., Brain Res Bull, 2005, 15;68(1-2):95-102.

8. Snykers S1, De Kock J, Tamara V, Rogiers V., “Hepatic differentiation of mesenchymal stem cells: in vitro strategies”., Methods Mol Biol. 2011; 698:305-14.

9. Lo, Bernard, and Lindsay Parham. “Ethical Issues in Stem Cell Research.” Endocrine Reviews, 2009, 30(3): 204–213.

10. Liu, Zhiqiang et al. “The Tumourigenicity of iPS Cells and Their Differentiated Derivates.” Journal of Cellular and Molecular Medicine, 2013, 17(6): 782–791.

11. Aldahmash A1, Atteya M, Elsafadi M, Al-Nbaheen M, Al-Mubarak HA, Vishnubalaji R, Al-Roalle A, Al-Harbi S, Manikandan M, Matthaei KI, Mahmood A., “Teratoma formation in immunocompetent mice after syngeneic and allogeneic implantation of germline capable mouse embryonic stem cells.”, Asian Pac J Cancer Prev. 2013, 14(10): 5705-11.

12. Wei, Xin et al. “Mesenchymal Stem Cells: A New Trend for Cell Therapy.” Acta Pharmacologica Sinica,

2013, 34(6): 747–754.

13. Kidd, Shannon et al. “Direct Evidence of Mesenchymal Stem Cell Tropism for Tumor and Wounding Microenvironments Using In Vivo Bioluminescence Imaging.” Stem cells (Dayton, Ohio), 2009, 27(10): 2614–2623.

14. Qinjun Zhaoa, Hongying Renb, Zhongchao Han, “Mesenchymal stem cells: Immunomodulatory capability and clinical potential in immune diseases”, Journal of Cellular Immunotherapy, 2016, 2(1): 3-20

15. Mao, Angelo S., and David J. Mooney. “Regenerative Medicine: Current Therapies and Future Directions.” Proceedings of the National Academy of Sciences of the United States of America, 2015,112(47): 14452–14459.

16. Gjorgieva D, Zaidman N, Bosnakovski D., “Mesenchymal stem cells for anti-cancer drug delivery.”, Recent Pat Anticancer Drug Discov, 2013, 8(3): 310-8.

17. Lee, Hwa-Yong, and In-Sun Hong. “Double-edged Sword of Mesenchymal Stem Cells: Cancer-promoting versus Therapeutic Potential.” Cancer Science, 2017, 108(10): 1939–1946.

18. Hou L, Wang X, Zhou Y, Ma H, Wang Z, He J, Hu H, Guan W, Ma Y., “Inhibitory effect and mechanism of mesenchymal stem cells on liver cancer cells.”, Tumour Biol. 2014, 35(2): 1239-50.

19. Xiao-Bing Wu, Yang Liu, Gui-Hua Wang, Xiao Xu, Yang Cai, Hong-Yi Wang, Yan-Qi Li, Hong-Fang Meng, Fu Dai & Ji-De Jin, “Mesenchymal stem cells promote colorectal cancer progression through AMPK/mTOR-mediated NF-κB activation”, Scientific Reports, 2016, 6(21420)

20. Akimoto, Keiko et al. “Umbilical Cord Blood-Derived Mesenchymal Stem Cells Inhibit, But Adipose Tissue-Derived Mesenchymal Stem Cells Promote, Glioblastoma Multiforme Proliferation.” Stem Cells and Development, 2013, 22(9): 1370–1386.

21. Jazedje, T. et al. “Human Mesenchymal Stromal Cells Transplantation May Enhance or Inhibit 4T1 Murine Breast Adenocarcinoma through Different Approaches.” Stem Cells International, 2015, 2015: 796215.

22. Nowakowski, Adam et al. “Engineered Mesenchymal Stem Cells as an Anti-Cancer Trojan Horse.” Stem Cells and Development, 2016, 25(20): 1513–1531.

23. Melzer, Catharina, Yuanyuan Yang, and Ralf Hass. “Interaction of MSC with Tumor Cells.” Cell Communication and Signaling : CCS, 2016, 14(1): 20.

24. Park, Ji Sun et al. “Engineering Mesenchymal Stem Cells for Regenerative Medicine and Drug Delivery.” Methods (San Diego, Calif.), 2015, 84: 3–16.

25. Kalimuthu, Senthilkumar et al. “Genetically Engineered Suicide Gene in Mesenchymal Stem Cells Using a Tet-On System for Anaplastic Thyroid Cancer.” Ed. Juri G. Gelovani. PLoS ONE, 2017, 12(7)

26. Pollock, Kari et al. “Human Mesenchymal Stem Cells Genetically Engineered to Overexpress Brain-Derived Neurotrophic Factor Improve Outcomes in Huntington’s Disease Mouse Models.” Molecular Therapy, 2016, 24(5): 965–977.

27 Geoffrey M Cooper, The Cell: A Molecular Approach. 2nd edition., 2000

28. Marino, Federica Zito, Marina Accardo, and Renato Franco. “CRISPR-Barcoding in Non Small Cell Lung Cancer: From Intratumor Genetic Heterogeneity Modeling to Cancer Therapy Application.” Journal of Thoracic Disease, 2017, 9(7): 1759–1762.

29. Gaj, Thomas, Charles A. Gersbach, and Carlos F. Barbas. “ZFN, TALEN and CRISPR/Cas-Based Methods for Genome Engineering.” Trends in biotechnology, 2013, 31(7): 397–405.

30. Eid, Ayman, and Magdy M Mahfouz. “Genome Editing: The Road of CRISPR/Cas9 from Bench to Clinic.” Experimental & Molecular Medicine, 2016, 48(10)

31. Raghavendrarao, Sanagala, Anil Kumar, Moola, Ranjitha Kumari, Bollipo Diana, “A review on advanced methods in plant gene targeting”, Journal of Genetic Engineering and Biotechnology, 2017, 15(2): 317-321

32. Sánchez-Rivera, Francisco J., and Tyler Jacks. “Applications of the CRISPR-Cas9 System in Cancer Biology.” Nature reviews. Cancer, 2015, 15(7): 387–395.

33. Jiang F, Doudna JA, “CRISPR-Cas9 Structures and Mechanisms.”, Annu Rev Biophys. 2017, 22(46): 505-529.

34. Ding, Yuduan et al. “Recent Advances in Genome Editing Using CRISPR/Cas9.” Frontiers in Plant Science, 2016, 7(703).

35. Ji Luo, “Genome Engineering to Cancer Drug Discovery.” Trends in cancer. 2016, 2(6): 313-324.

36. Chen, Si et al. “CRISPR-Cas9: From Genome Editing to Cancer Research.” International Journal of Biological Sciences, 2016, 12(12): 1427–1436.

37. Han, Xin et al. “CRISPR-Cas9 Delivery to Hard-to-Transfect Cells via Membrane Deformation.” Science Advances, 2015, 1(7)

38. Kouranova, Evguenia et al. “CRISPRs for Optimal Targeting: Delivery of CRISPR Components as DNA, RNA, and Protein into Cultured Cells and Single-Cell Embryos.” Human Gene Therapy, 2016, 27(6): 464–475.

39. Mali, Prashant et al. “RNA-Guided Human Genome Engineering via Cas9.” Science (New York, N.Y.), 2013, 339(6121): 23–826.

40. Papapetrou, Eirini P, and Axel Schambach. “Gene Insertion Into Genomic Safe Harbors for Human Gene Therapy.” Molecular Therapy, 2016, 24(4): 678–684.

41. Roberts, Brock et al. “Systematic Gene Tagging Using CRISPR/Cas9 in Human Stem Cells to Illuminate Cell Organization.” Ed. David G. Drubin. Molecular Biology of the Cell, 2017, 28(21): 2854–2874.

42. Anders, Carolin, and Martin Jinek. “In Vitro Enzymology of Cas9.” Methods in enzymology, 2014, 546: 1–20.

43. Redman, Melody et al. “What Is CRISPR/Cas9?” Archives of Disease in Childhood. Education and Practice Edition, 2016,101(4): 213–215.

44. Dai WJ, Zhu LY, Yan ZY, Xu Y, Wang QL, Lu XJ. CRISPR-Cas9 for in vivo Gene Therapy: Promise and Hurdles. Mol Ther Nucleic Acids, 2016, 5(8) 45. Larijani B, Esfahani EN, Amini P, Nikbin B, Alimoghaddam K, Amiri S, Malekzadeh R, Yazdi NM, Ghodsi M, Dowlati Y, Sahraian MA, Ghavamzadeh A., “Stem cell therapy in treatment of different diseases”., Acta Med Iran. 2012, 50(2): 79-96.

46. Mount, Natalie M. et al. “Cell-Based Therapy Technology Classifications and Translational Challenges.” Philosophical Transactions of the Royal Society B: Biological Sciences, 2015, 370(1680): 20150017.

47. Shimizu-Motohashi, Yuko et al. “Recent Advances in Innovative Therapeutic Approaches for Duchenne Muscular Dystrophy: From Discovery to Clinical Trials.” American Journal of Translational Research, 2016, 8(6): 2471–2489.

48. Tabebordbar, Mohammadsharif et al. “In Vivo Gene Editing in Dystrophic Mouse Muscle and Muscle Stem Cells.” Science (New York, N.Y.), 2016, 351(6271): 407–411.

49. Long, Chengzu et al. “Postnatal Genome Editing Partially Restores Dystrophin Expression in a Mouse Model of Muscular Dystrophy.” Science (New York, N.Y.), 2016, 351(6271): 400–403.

50. Long, Chengzu et al. “Prevention of Muscular Dystrophy in Mice by CRISPR/Cas9–mediated Editing of Germline DNA.” Science (New York, N.Y.), 2014, 345(6201): 1184–1188.

51. Firth, Amy L et al. “Functional Gene Correction for Cystic Fibrosis in Lung Epithelial Cells Generated From Patient iPSCs.” Cell reports, 2015, 12(9): 1385–1390.

52. Sanz, David J. et al. “Cas9/gRNA Targeted Excision of Cystic Fibrosis-Causing Deep-Intronic Splicing Mutations Restores Normal Splicing of CFTR mRNA.” Ed. Emanuele Buratti. PLoS ONE, 2017, 12(9)

53. Gerald Schwank, Bon-Kyoung Koo, Valentina Sasselli, Johanna F. Dekkers, Inha Heo, Turan Demircan, Nobuo Sasaki, Sander Boymans, Edwin Cuppen, Cornelis K. van der Ent, et al.,”Functional repair of CFTR by CRISPR/Cas9 in intestinal stem cell organoids of cystic fibrosis patients.”Cell Stem Cell., 2013, 13(6): 653-8

54. García-Tuñón, Ignacio et al. “The CRISPR/Cas9 System Efficiently Reverts the Tumorigenic Ability of BCR/ABL in Vitro and in a Xenograft Model of Chronic Myeloid Leukemia.” Oncotarget, 2017, 8(16): 26027–26040.

55. Brabetz, Oliver et al. “RNA-Guided CRISPR-Cas9 System-Mediated Engineering of Acute Myeloid Leukemia Mutations.” Molecular Therapy. Nucleic Acids, 2017, 17(6): 243–248.

56. Xue Gao, Yong Tao, Veronica Lamas, Mingqian Huang, Wei-Hsi Yeh, Bifeng Pan, Yu-Juan Hu, Johnny H. Hu, David B. Thompson, Yilai Shu, Yamin Li, Hongyang Wang, Shiming Yang, Qiaobing Xu, et al, Treatment of autosomal dominant hearing loss by in vivo delivery of genome editing agents, Nature, 2018, 553: 217-221

57. Glenn Yiu, MD, PhD, “Genome Editing in Retinal Diseases using CRISPR Technology”, Department of Ophthalmology & Vision Science, University of California, Davis, Sacramento, California, 2018, 2(1): 1–3

58. Yu, Wenhan et al. “Nrl Knockdown by AAV-Delivered CRISPR/Cas9 Prevents Retinal Degeneration in Mice.” Nature Communications, 2017, 8(14716).

59. Glenn Yiu, MD, PhD, “Genome Editing in Retinal Diseases using CRISPR Technology”, Department of Ophthalmology & Vision Science, University of California, Davis, Sacramento, California, 2018, 2(1): 1–3

60. Suzuki, Keiichiro et al. “In Vivo Genome Editing via CRISPR/Cas9 Mediated Homology-Independent Targeted Integration.” Nature, 2016, 540(7631): 144–149.

61. Pastor JC, “Proliferative vitreoretinopathy: an overview.”, Surv Ophthalmol., 1998, 43(1): 3-18.

62. Xu CL, Park KS, Tsang SH, “CRISPR/Cas9 genome surgery for retinal diseases.”, Drug Discov Today Technol., 2018, 28: 23-32.

63. Ortiz-Virumbrales, Maitane et al. “CRISPR/Cas9-Correctable Mutation-Related Molecular and Physiological Phenotypes in iPSC-Derived Alzheimer’s PSEN2N141I Neurons.” Acta Neuropathologica Communications, 2017, 5(77).

64. Zhen S, Li X, “Oncogenic Human Papillomavirus: Application of CRISPR/Cas9 Therapeutic Strategies for Cervical Cancer”. Cell Physiol Biochem., 2017, 44(6): 2455-2466

65. Kennedy, Edward M. et al. “Inactivation of the Human Papillomavirus E6 or E7 Gene in Cervical Carcinoma Cells by Using a Bacterial CRISPR/Cas RNA-Guided Endonuclease.” Ed. R. M. Sandri-Goldin. Journal of Virology, 2014, 88(20): 11965–11972.

66. Zheng Hu, Lan Yu, Da Zhu, Wencheng Ding, Xiaoli Wang, Changlin Zhang, Liming Wang, Xiaohui Jiang, Hui Shen, Dan He, Kezhen Li, Ling Xi, Ding Ma, and Hui Wang, “Disruption of HPV16-E7 by CRISPR/Cas System Induces Apoptosis and Growth Inhibition in HPV16 Positive Human Cervical Cancer Cells”, BioMed Research International, 2014, 2014: 9

67. Lin, Guigao, Kuo Zhang, and Jinming Li. “Application of CRISPR/Cas9 Technology to HBV.” Ed. Izuho Hatada. International Journal of Molecular Sciences, 2015, 16(11): 26077–26086.

68. Wang, Jie et al. “Dual gRNAs Guided CRISPR/Cas9 System Inhibits Hepatitis B Virus Replication.” World Journal of Gastroenterology: WJG, 2015, 21(32): 9554–9565.

69. Ramanan, Vyas et al. “CRISPR/Cas9 Cleavage of Viral DNA Efficiently Suppresses Hepatitis B Virus.” Scientific Reports, 2015, 5(10833).

70. S. Zhen, L. Hua, Y-H Liu, L-C Gao, J. Fu, D-Y Wan, L-H Dong, H-F Song, X. Gao, “Harnessing the clustered regularly interspaced short palindromic repeat (CRISPR)/CRISPR-associated Cas9 system to disrupt the hepatitis B virus.” Gene Ther. 2015; 22(5): 404–412.

71. Kennedy EM, Kornepati AV, Cullen BR, “Targeting hepatitis B virus cccDNA using CRISPR/Cas9.”, Antiviral Res., 2015, 123: 188-92.

72. Karimova, Madina et al. “CRISPR/Cas9 Nickase-Mediated Disruption of Hepatitis B Virus Open Reading Frame S and X.” Scientific Reports, 2015, 5(13734).

73. Li, Hao et al. “Removal of Integrated Hepatitis B Virus DNA Using CRISPR-Cas9.” Frontiers in Cellular and Infection Microbiology, 2017, 7(91).

74. Kit-San Yuen, Chi-Ping Chan, Nok-Hei Mickey Wong, Chau-Ha Ho, Ting-Hin Ho, Ting Lei, Wen Deng, Sai Wah Tsao, Honglin Chen, Kin-Hang Kok, et al. “CRISPR/Cas9-mediated genome editing of Epstein-Barr virus in human cells”. J Gen Virol., 2015; 96(Pt 3): 626–636.

75. Wang, Jianbin, and Stephen R. Quake. “RNA-Guided Endonuclease Provides a Therapeutic Strategy to Cure Latent Herpesviridae Infection.” Proceedings of the National Academy of Sciences of the United States of America, 2014, 111(36): 13157–13162.

76. Yajima M, Ikuta K, Kanda T. Rapid CRISPR/Cas9-Mediated Cloning of Full-Length Epstein-Barr Virus Genomes from Latently Infected Cells. Viruses. 2018, 10(4): 171.

77. Yuen KS, Chan CP, Kok KH, Jin DY, “Mutagenesis and Genome Engineering of Epstein-Barr Virus in Cultured Human Cells by CRISPR/Cas9.”, Methods Mol Biol., 2017, 1498: 23-31.

78. Karn, Jonathan, and C. Martin Stoltzfus. “Transcriptional and Posttranscriptional Regulation of HIV-1 Gene Expression.” Cold Spring Harbor Perspectives in Medicine, 2012, 2(2)

79. Lebbink, Robert Jan et al. “A Combinational CRISPR/Cas9 Gene-Editing Approach Can Halt HIV Replication and Prevent Viral Escape.” Scientific Reports, 2017, 7(41968).

80. Ebina, Hirotaka et al. “Harnessing the CRISPR/Cas9 System to Disrupt Latent HIV-1 Provirus.” Scientific Reports, 2013, 3(2510).

81. Kaminski, Rafal et al. “Elimination of HIV-1 Genomes from Human T-Lymphoid Cells by CRISPR/Cas9 Gene Editing.” Scientific Reports, 2016, 6(22555).

82. Yin C, Zhang T, Qu X, Zhang Y, Putatunda R, Xiao X, Li F, Xiao W, Zhao H, Dai S, Qin X, Mo X, Young WB, Khalili K, Hu W.” In Vivo Excision of HIV-1 Provirus by saCas9 and Multiplex Single-Guide RNAs in Animal Models.”, Mol Ther., 2017, 3;25(5):1168-1186

83. Wang Z, Pan Q, Gendron P, Zhu W, Guo F, Cen S, Wainberg MA, Liang C, “CRISPR/Cas9-Derived Mutations Both Inhibit HIV-1 Replication and Accelerate Viral Escape.”, Cell Rep., 2016, 19;15(3):481-489.

84. Marino, Federica Zito, Marina Accardo, and Renato Franco. “CRISPR-Barcoding in Non Small Cell Lung Cancer: From Intratumor Genetic Heterogeneity Modeling to Cancer Therapy Application.” Journal of Thoracic Disease, 2017, 9(7): 1759–1762.

85. Aldarouish, Mohanad, and Cailian Wang. “Trends and Advances in Tumor Immunology and Lung Cancer Immunotherapy.” Journal of Experimental & Clinical Cancer Research: CR, 2016, 35(157).

86. David Cyranoski, “CRISPR gene editing tested in a person”, Nature news, 24 November 2016, Vol 539

87. Wei C, Wang F, Liu W, et al. CRISPR/Cas9 targeting of the androgen receptor suppresses the growth of LNCaP human prostate cancer cells. Molecular Medicine Reports. 2018, 17(2): 2901-2906.

88. Fei, Teng et al. “Genome-Wide CRISPR Screen Identifies HNRNPL as a Prostate Cancer Dependency Regulating RNA Splicing.” Proceedings of the National Academy of Sciences of the United States of America, 2017,114(26): 5207–5215.

89. Zhen, Shuai et al. “Targeted Delivery of CRISPR/Cas9 to Prostate Cancer by Modified gRNA Using a Flexible Aptamer-Cationic Liposome.” Oncotarget, 2017, 8(6): 9375–9387.

90. Chen, Zhang-Hui et al. “Targeting Genomic Rearrangements in Tumor Cells Using Cas9-Mediated Insertion of a Suicide Gene.” Nature biotechnology, 2017, 35(6): 543–550.

91. Haitao Yang, MariaLynn Jaeger, Averi Walker, Daniel Wei, Katie Leiker, Tao Weitao, “Break Breast Cancer Addiction by CRISPR/Cas9 Genome Editing”, J Cancer, 2018, 9(2): 219-231

92. Annunziato, Stefano et al. “Modeling Invasive Lobular Breast Carcinoma by CRISPR/Cas9-Mediated Somatic Genome Editing of the Mammary Gland.” Genes & Development, 2016, 30(12): 1470–1480.

93. Zara Kassam, “NEWS CRISPR-dCas9 reveals surprising insight into breast cancer development”, Drug Target Review, 2017

94. Elaine K. Howley, “What Might CRISPR and Gene Editing Mean for Breast Cancer?”, USNews, 2017

95. Anelli V, Villefranc JA, Chhangawala S, et al. Oncogenic BRAF disrupts thyroid morphogenesis and function via twist expression. Green MR, ed. eLife. 2017, 6(20728).

96. Jafari, Naser et al. “CRISPR-Cas9 Mediated NOX4 Knockout Inhibits Cell Proliferation and Invasion in HeLa Cells.” Ed. Guei-Sheung Liu. PLoS ONE, 2017, 12(1)

97. Huang X, Zhuang C, Zhuang C, Xiong T, Li Y, Gui Y., “An enhanced hTERT promoter-driven CRISPR/Cas9 system selectively inhibits the progression of bladder cancer cells.”, Mol Biosyst., 2017, 13(9): 1713-1721

98. Liu Y, Zeng Y, Liu L, Zhuang C, Fu X, Huang W, Cai Z, “Synthesizing AND gate genetic circuits based on CRISPR-Cas9 for identification of bladder cancer cells.”, Nat Commun., 2014, 5(5393)

99. Chen, Zhicong et al. “Recent Development on Synthetic Biological Devices Treating Bladder Cancer.” Synthetic and Systems Biotechnology, 2016, 1(4): 216–220.

100. Jef Ekins “CRISPR-Cas9 technique exploits pancreatic cancer cells' vulnerabilities to develop new treatments”, nature medicine news, University of Toronto, 2016

101. Ren, Jiangtao, and Yangbing Zhao. “Advancing Chimeric Antigen Receptor T Cell Therapy with CRISPR/Cas9.” Protein & Cell, 2017, 8(9): 634–643.

102. Zhang Y, Zhang X, Cheng C, Mu W, Liu X, Li N, Wei X, Liu X, Xia C, Wang H8, “CRISPR-Cas9 mediated LAG-3 disruption in CAR-T cells.”, Front Med., 2017, 11(4): 554-562

103. Ella Marushchenko, “CRISPR-SMART Cells Regenerate Cartilage, Secrete Anti-Arthritis Drug”, GEN News Highlights, 2017.

104. Brunger, Jonathan M. et al. “Genome Engineering of Stem Cells for Autonomously Regulated, Closed-Loop Delivery of Biologic Drugs.” Stem Cell Reports, 2017, 8(5) 1202–1213.

105. Yamada, Tohru et al. “The Bacterial Redox Protein Azurin Induces Apoptosis in J774 Macrophages through Complex Formation and Stabilization of the Tumor Suppressor Protein p53.” Infection and Immunity, 2002, 70(12): 7054–7062.

106. Punj V, Bhattacharyya S, Saint-Dic D, Vasu C, Cunningham EA, Graves J, Yamada T, Constantinou AI, Christov K, White B, Li G, Majumdar D, Chakrabarty AM, Das Gupta TK., “Bacterial cupredoxin azurin as an inducer of apoptosis and regression in human breast cancer.”, Oncogene., 2004, 23(13): 2367-78.

107. Yamada T, Fialho AM, Punj V, Bratescu L, Gupta TK, Chakrabarty AM., “Internalization of bacterial redox protein azurin in mammalian cells: entry domain and specificity.”, Cell Microbiol. 2005, 7(10):1418-31.

108. Rajeshwari R. Mehta, Tohru YamadaBrad N. Taylor, Konstantin Christov, Marissa L. King, Dibyen Majumdar, Fatima Lekmine, Chinnaswamy Tiruppathi, Anne Shilkaitis, Laura Bratescu, Albert Green, Craig W. Beattie, Tapas K. Das Gupta,” A cell penetrating peptide derived from azurin inhibits angiogenesis and tumor growth by inhibiting phosphorylation of VEGFR-2, FAK and Akt”, 2011, 14(3): 355–369

109. Bernardes, Nuno et al. “The Bacterial Protein Azurin Impairs Invasion and FAK/Src Signaling in P-Cadherin-Overexpressing Breast Cancer Cell Models.” Ed. Claudia Daniela Andl. PLoS ONE, 2013, 8(7)

110. Chaudhari A, Mahfouz M, Fialho AM, Yamada T, Granja AT, Zhu Y, Hashimoto W, Schlarb-Ridley B, Cho W, Das Gupta TK, Chakrabarty AM., “Cupredoxin-cancer interrelationship: azurin binding with EphB2,

interference in EphB2 tyrosine phosphorylation, and inhibition of cancer growth.", Biochemistry. 2007, 20;46(7): 1799-810.

111. Ananda M. Chakrabarty, "Bacterial azurin in potential cancer therapy", CELL CYCLE, 2016, 15(13): 1665–1666

112. Tropea JE, Cherry S, Waugh DS., "Expression and purification of soluble His(6)-tagged TEV protease.", Methods Mol Biol., 2009, 498: 297-307

113. Madeira C, Ribeiro SC, Pinheiro IS, Martins SA, Andrade PZ, da Silva CL, Cabral JM., "Gene delivery to human bone marrow mesenchymal stem cells by microporation.," Journal of Biotechnology, 2011, 151(1): 130-6

114. Robichon, Carine et al. "Engineering Escherichia Coli BL21(DE3) Derivative Strains To Minimize E. Coli Protein Contamination after Purification by Immobilized Metal Affinity Chromatography." Applied and Environmental Microbiology, 2011, 77(13): 4634–4646.

115. Fuguo Jiang, Jennifer A. Doudna, "CRISPR–Cas9 Structures and Mechanisms", Annual Review of Biophysics, 2017, 46: 505-529

116. Peters JM, Silvis MR, Zhao D, Hawkins JS, Gross CA, Qi LS. "Bacterial CRISPR: Accomplishments and Prospects." Current opinion in microbiology. 2015; 27: 121-126.

117. Malakar P, Venkatesh KV., "Effect of substrate and IPTG concentrations on the burden to growth of Escherichia coli on glycerol due to the expression of Lac proteins.", Appl Microbiol Biotechnol., 2012, 93(6): 2543-9.

118. Shcherbakova, Daria M., Oksana M. Subach, and Vladislav V. Verkhusha. "Red Fluorescent Proteins: Advanced Imaging Applications and Future Design." Angewandte Chemie (International ed. in English), 2012, 51(43): 10724–10738.

119. Berezin, Mikhail Y., Jeff Kao, and Samuel Achilefu. "pH-Dependent Optical Properties of Synthetic Fluorescent Imidazoles." Chemistry (Weinheim an der Bergstrasse, Germany), 2009, 15(14): 3560–3566.

120. Doherty, Geoff P, Kirra Bailey, and Peter J Lewis. "Stage-Specific Fluorescence Intensity of GFP and mCherry during Sporulation In Bacillus Subtilis." BMC Research Notes, 2010, 3(303).

121. Halim, Nur Shuhaidatul Sarmiza Abdul et al. "A Comparative Study of Non-Viral Gene Delivery Techniques to Human Adipose-Derived Mesenchymal Stem Cell." International Journal of Molecular Sciences, 2014, 15(9): 15044–15060.

8. Annexes

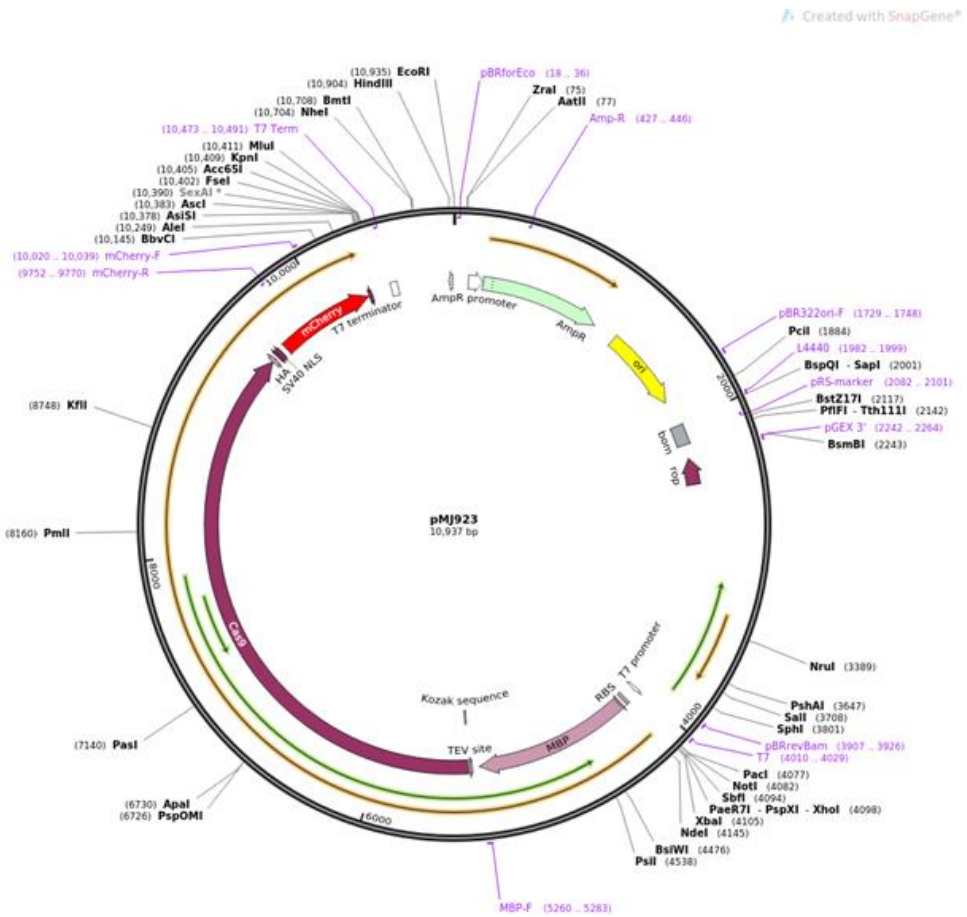

Figure A1: pMJ923 plasmid structure. Acquired from Addgene at # 78313. Used in 6 His-MBP-Cas9-mCherry expression.

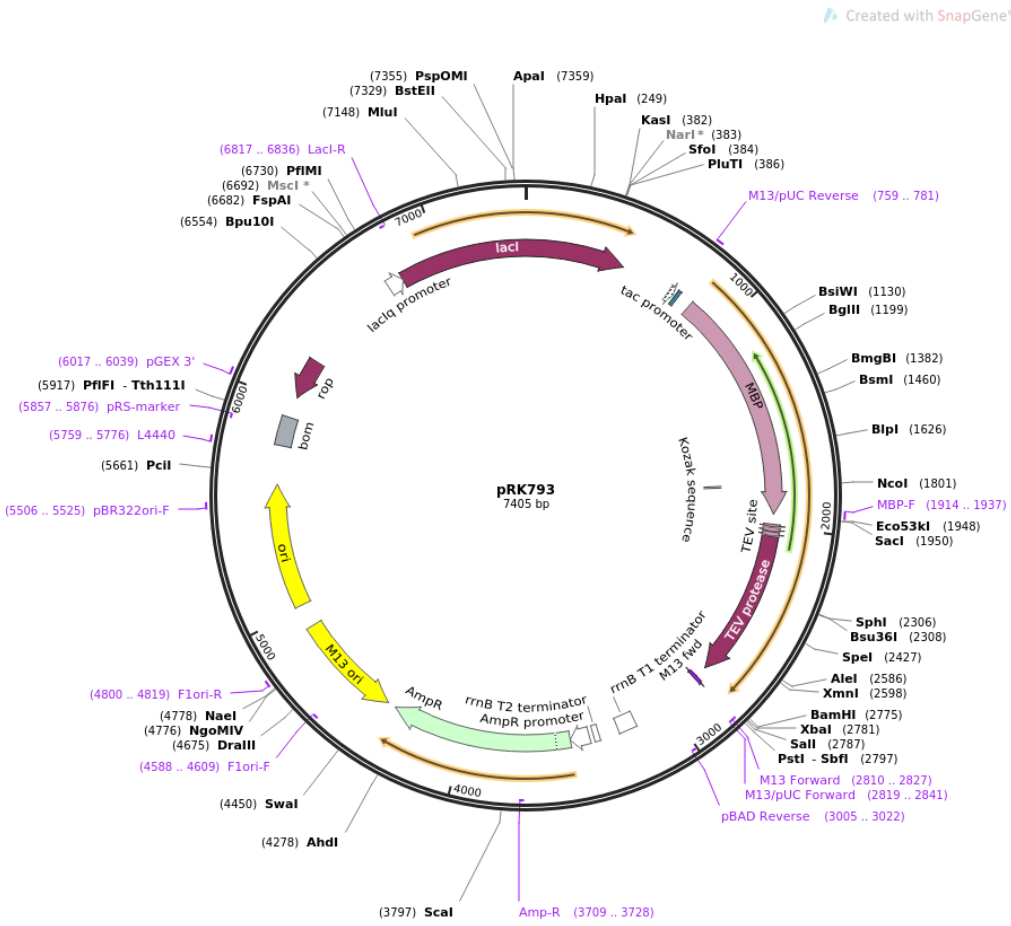

Figure A2: pRK793 plasmid structure. Acquired from Addgene at #8827. Used for TEV expression.

Figure A3: pX458 plasmid structure. Acquired from Addgene at # 48138). Used for all-in-one plasmid approach.

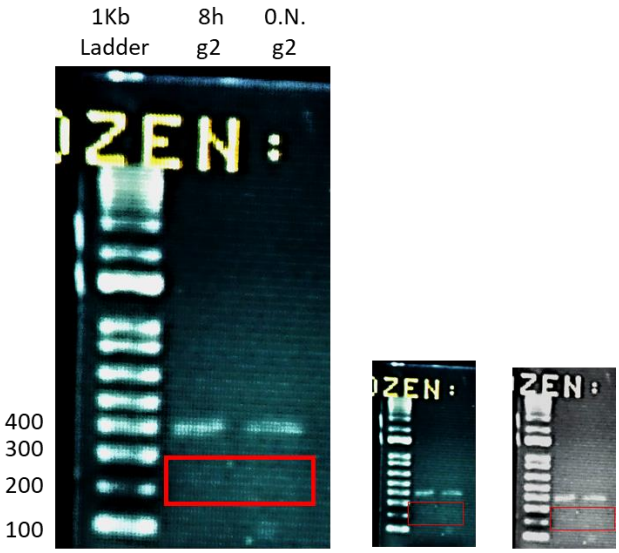

Figure A4: 1.2% Agarose gel of CRISPR-Cas9 cleavage assay in the PCR product of target region of MSCs. Cleavage with guide2 with incubation with RNP and Lipofectamine 2000 for 8h and overnight. The miniatures of the gel are meant to see more clearly the very tenue bands close to 200 bp that indicate very low efficiency of cleavage and transfection.